What is It Like to be a Crab? A Complex Network Analysis of Eucaridan Evolution

Agustín Ostachuk

Evolutionary Biology

ISSN 0071-3260
Volume 46
Number 2

Evol Biol (2019) 46:179-206
DOI 10.1007/s11692-019-09475-9

Springer

Evolutionary Biology (2019) 46:179–206
https://doi.org/10.1007/s11692-019-09475-9

RESEARCH ARTICLE

What is It Like to be a Crab? A Complex Network Analysis of Eucaridan Evolution

Agustín Ostachuk[1,2]

Received: 13 July 2018 / Accepted: 23 April 2019 / Published online: 2 May 2019

Abstract

Eucaridan evolution involved a process starting from a body organization characterized by an elongate and cylindrical cephalothorax, a well-developed abdomen composed of swimming appendages, ending in a tail fan formed by flattened uropods and a telson. This process would lead, ultimately, to a body organization characterized by a shortened and depressed cephalothorax, and a reduced and ventrally folded abdomen. This ultimate process is typically known as carcinization, and is commonly defined as the process of becoming a crab. In this work, the evolution of the superorder Eucarida was studied using complex networks. A new definition of crab and carcinization are given based on the results obtained. A crab is a topological structural closure that determines the formation of a triadic central core. The evolution of the crab implied the formation of a triadic structure with high closeness centrality, formed by the cephalon, the fused thoracomere 1–4 and the carapace, which represented a highly stable hierarchical core deeply buried or enclosed in the topological structure of the network, responsible for the generation of a highly integrated and robust topology. Under this new definition, the representative of the infraorder Anomura used in this work, which is commonly considered as a crab, is not. This network seemed to be characterized by the presence of a quasi-dyadic structure, formed by the cephalon and the carapace, which was not sufficient for generating the topological closure.

Keywords Theoretical biology · Evo-devo · Complexity · Network theory

Introduction

It is generally acknowledged that eucaridan evolution involved a process starting from a body organization characterized by an elongate and cylindrical cephalothorax, a well-developed, articulated and sclerotized abdomen (or pleon) composed of swimming appendages, and ending in a tail fan formed by flattened uropods and a telson, a condition typically found in what are commonly referred as shrimps. On the other hand, this process would lead, ultimately, to a body organization characterized by a shortened and depressed cephalothorax and a reduced, diminished and ventrally folded abdomen, a condition found in what are commonly referred as crabs. This ultimate process is typically known as carcinization (McLaughlin and Lemaitre 1997) and it is considered one of the main examples of evolutionary convergence (Scholtz 2014).

It is clear from the above that the main event in eucaridan evolution was carcinization. As carcinization is defined as the process of becoming a crab, it creates consequently the problem of defining what a crab is. Various definitions of what a crab is were given through history, although ultimately they are all reduced to the same principles. Borradaile, who was the first to propose the term carcinization, defined it as "a reduction of the abdomen of a macrurous crustacean, together with a depression and broadening of its cephalothorax, so that the animal assumes the general habit of body of a crab" (Borradaile 1916). More recently, Martin and Abele defined carcinization as the "reduction and folding of the abdomen beneath the thorax" (Martin and Abele 1986). Meanwhile, Scholtz

Electronic supplementary material The online version of this article (https://doi.org/10.1007/s11692-019-09475-9) contains supplementary material, which is available to authorized users.

✉ Agustín Ostachuk
aostachuk@unsam.edu.ar

[1] Museo de La Plata (MLP), Universidad Nacional de La Plata (UNLP), Buenos Aires, Argentina

[2] Centro de Estudios de Historia de la Ciencia y de la Técnica José Babini, Universidad Nacional de San Martín (UNSAM), Buenos Aires, Argentina

defined a decapod crustacean as a crab when the following criteria were fulfilled: "carapace depressed with lateral margin; carapace with similar width and length; sternum wide; pleon ventrally flexed" (Scholtz 2014). As can be seen, all the definitions point to the same morphological features: they all define a crab based on the fulfillment of certain geometrical and sizeable characteristics.

A novel method for biological analysis is network theory (Newman 2003; Boccaletti et al. 2006; Mason and Verwoerd 2007). A network is a set of items, called vertices or nodes, with connections between them, called edges. The typical representation of a network is a series of dots (nodes) connected by lines (edges). The fundamental characteristic of network theory is that many systems in nature and culture can be abstracted as networks. Network theory has been used to model the structure and behavior of many biological processes: neural networks, metabolic networks, protein interaction networks, food-webs, social networks, etc. These diverse applications have demonstrated that networks and complex systems share various structural properties that determine their global behavior, such as the presence of small-world effect, scale-free distribution, community structure and tolerance to errors (Boccaletti et al. 2006).

Diego Rasskin-Gutman and Borja Esteve-Altava have pioneered the use of network theory in anatomical systems, focusing on the study of tetrapod skulls, in what they have called Anatomical Network Analysis (AnNA) (Rasskin-Gutman and Esteve-Altava 2014). Firstly, Diego Rasskin-Gutman used network theory for the exploration of the theoretical morphospace of archosaurs pelvic girdles (Rasskin-Gutman and Buscalioni 2001). Then, they studied the modularity and integration of the human skull (Esteve-Altava et al. 2013b), and the structural constraints in the evolution of tetrapod skulls (Esteve-Altava et al. 2013a). Recently, they have extended their anatomical network analysis in order to study the musculoskeletal system of the human head (Esteve-Altava et al. 2015). With the aid of network analysis, they were able to show that the human skull is a small-world network, consisting of two connectivity modules (Esteve-Altava et al. 2013b). Moreover, they were able to show that the reduction of bones in tetrapod skulls, an evolutionary trend known as "Williston's Law", is accompanied by an increase in morphological complexity (Esteve-Altava et al. 2013a). These studies have shown the potential of complex networks to reveal new phenomena in the process of cranial evolution. They have demonstrated the existence of structural properties in skulls, not accessible to more traditional methods for the study of morphological evolution (i.e. geometric morphometrics). While the latter are based on the concept of shape, the former are based on the concept of connectivity. They represent different "levels of morphological information" that allow the identification of "level-specific processes" (Rasskin-Gutman and Esteve-Altava 2014).

In this work, I studied the evolution of the superorder Eucarida (Malacostraca) using complex networks. The most characteristic representatives of the superorder were modeled as networks and their characteristics were analyzed. I propose a new definition of a crab based on the results obtained. The evolution of the crab in the superorder Eucarida implied an "enclosure", but not of the abdomen beneath the thorax. The evolution of the crab implied the formation of a triadic structure with high closeness centrality, formed by the cephalon, the fused thoracomere 1–4 and the carapace, which represented a highly stable core deeply buried or enclosed in the topological structure of the network. Under this new definition, the representative of the infraorder Anomura used in this work, which is commonly considered as a crab, is not. This network seemed to be characterized by the presence of a quasi-dyadic structure, formed by the cephalon and the carapace, which was not sufficient for generating the topological closure.

Materials and Methods

The Crustacean Network Model

The external morphology of crustaceans were modeled using network theory. All morphological features clearly identifiable and distinguishable as individual units were abstracted as nodes. In this manner, segments, articles, endites, exites, and epipods were considered nodes. Flagella were abstracted as single nodes. The only morphological feature not considered for the analysis was setae, which are hair-like processes from the cuticle. When the external morphology was not enough for the determination of a clear delimitation between segments, information from the internal morphology, such as the endoskeleton and musculature, was studied and considered in the analysis for a final decision. On the other hand, physical connections between the individual units defined above (nodes) were considered as edges.

In this work, the evolution of the superorder Eucarida (Malacostraca) was studied. The majority of the groups belonging to the superorder were modeled as networks. These groups, ordered in evolutionary sequence, were the following (representative genera in parentheses): Euphausiacea (*Euphausia*) (Spiridonov and Casanova 2010; Maas and Waloszek 2001), Dendrobranchiata (*Penaeus*) (Young 1959), Caridea (*Pandalus*, complemented with *Palaemon*) (Berkeley 1928; Garm 2004; Garm et al. 2003), Astacidea (*Astacus*, complemented with *Homarus*) (Huxley 1880; Lavalli and Factor 1992; Wahle et al. 2012), Palinura (*Palinurus*) (Lavalli and Spanier 2010; Parker and Rich 1893), Anomura (*Aegla*) (Martin and Abele 1988; Tudge et al.

2012; Moraes et al. 2015; Snodgrass 1950) and Brachyura (*Callinectes* and *Portunus*) (Davie et al. 2015; Cochran 1935; Thoma et al. 2012; Freitag 2012). This order is congruent with the overall evolutionary trend found in the superorder, that is, from an elongate cephalothorax and a well-developed abdomen (pleon), to a shortened cephalothorax and a reduced and ventrally folded abdomen. This order is also supported by phylogenetic analysis (Dixon et al. 2003). The information necessary for the construction of the crustacean network models was obtained from specialized bibliography. The main references are cited above after each eucaridan group, although many others were studied and considered.

Once individual units and their connections were clearly defined, the information corresponding to nodes and edges was coded in a square matrix $N \times N$, where N was the total number of nodes of the network (adjacency matrix). Edges were coded following the binary code: 1 for the presence of connection, and 0 for the absence of connection (Newman 2003; Boccaletti et al. 2006; Mason and Verwoerd 2007). The adjacency matrices generated for the different groups of eucaridan evolution are provided as Supplementary Material.

Network Parameters

Average Degree

Node degree (k) is the number of connections of a particular node. The average degree is the mean of all node degrees. Meanwhile, the degree distribution, that is, the frequency of nodes with a certain degree, gives information about the network organization and enables to determine its basic properties.

Average Path Length

Path length is the distance that separates two nodes, that is, the number of edges that must be crossed in order to go from one to the other. The average path length (L) is the arithmetic mean of all the path lengths.

Average Clustering Coefficient

The clustering coefficient characterizes the density of connections in the surroundings of a node. It represents the ratio between the number of edges linked to their proximate neighbors, and the number of all possible edges among those proximate neighbors. The average clustering coefficient (C) is the mean of the clustering coefficient of all nodes.

Network Density

Network density describes the relation between actual connections (AC) and potential connections (PC) in a network. A potential connection is a connection between two nodes that could potentially exist, regardless of whether or not it actually does. It represents the total number of potential connections in the network.

Modularity

The identification of modules was made using multi-level optimization of modularity (Blondel et al. 2008). Community structure detection by multi-level optimization of modularity is based on the modularity measure (Q-value) (Newman and Girvan 2004) and a hierarchical approach. Initially, each node is assigned to a different community. Then, for each node it is considered the gain of modularity that would occur by placing it in the different neighboring communities. The node is re-assigned to the community to which contributes to the highest value of modularity. This process is repeated iteratively and stops when the modularity can no longer be increased.

Hierarchical Organization

Topological Overlap Analysis

The identification of the hierarchical organization was made using topological overlap (TO) (Ravasz et al. 2002). The topological overlap (O_T) is a normalized measure of interconnectedness and relatedness that quantifies common neighbors between pairs of nodes.

$$O_T(i,j) = \frac{J_n(i,j)}{min(k_i, k_j)},$$

where $J_n(i,j)$ is the number of nodes to which i and j are linked, and $min(k_i, k_j)$ is the smaller degree of i and j. Two nodes connected to the same nodes will have a topological overlap of 1, whereas two nodes sharing no connections will have a topological overlap of 0.

Functionality

Within-Module Degree and Participation Coefficient

This approach (Guimera and Amaral 2005) is based on the idea that nodes with the same role should have similar topological properties. The position of a node within its own module and with respect to the other modules are determined by two parameters: the within-module degree and the participation coefficient. The within-module degree (z_i) measures the

connectivity of a node to the other nodes in a given module. The participation coefficient (P_i) measures the distributivity of the links of a node among the different modules. P_i is close to 1 if the links are distributed uniformly among the modules, and 0 if they are all within its own module.

The within-module degree is calculated as:

$$z_i = \frac{k_i - \bar{k}_{s_i}}{\sigma_{k_{s_i}}},$$

where k_i is the number of links of node i to the other nodes in its module s_i, $\bar{k}_{s_i}$ is the average of k over all the nodes in s_i, and $\sigma_{k_{s_i}}$ is the standard deviation of k in s_i.

The participation coefficient is calculated as:

$$P_i = 1 - \sum_{s=1}^{N_M} \left(\frac{k_{is}}{k_i}\right)^2,$$

where k_{is} is the number of links of node i to nodes in module s and k_i is the total degree of node i.

Complexity Measures

Product Measures

Medium Articulation (*MAg*). Medium articulation (*MA*) is an information theoretic measure that tends to solve the issue regarding what kind of network is more stable: highly connected networks or less connected networks.

$$MA = R \cdot I,$$

where R is the redundancy and I is the mutual information.

For unweighted undirected networks they are calculated as:

$$R = 1/m \sum_{i,j>i} \log(k_i k_j), \quad I = 1/m \sum_{i,j>i} \log(2m/(k_i k_j)),$$

where m is the total number of edges of the network, and d_i and d_j are the node degrees of the considered edge.

MAg is the generalized form of *MA* and fulfills the condition $0 \leq MAg \leq 1$. It is calculated as:

$$MAg = MA_R \cdot MA_I,$$

where

$$MA_R = 4\left(\frac{R - R_{path}}{R_{clique} - R_{path}}\right)\left(1 - \frac{R - R_{path}}{R_{clique}}\right),$$
$$MA_I = 4\left(\frac{I - I_{clique}}{I_{path} - I_{clique}}\right)\left(1 - \frac{I - I_{clique}}{I_{path} - I_{clique}}\right).$$

Efficiency Complexity (*Ce*). The efficiency of a network is a measure of how efficiently it exchanges information (Latora and Marchiori 2001). The efficiency of a network can be defined as the arithmetic mean of all inverse shortest path lengths:

$$E = \frac{1}{N(N-1)/2} \sum_i \sum_{j>1} \frac{1}{d_{ij}},$$

where d_{ij} is the shortest path length between the nodes i and j.

The efficiency complexity (*Ce*) is a modified and normalized form of E ($0 \leq Ce \leq 1$) and is calculated as:

$$Ce = 4\left(\frac{E - E_{path}}{1 - E_{path}}\right)\left(1 - \frac{E - E_{path}}{1 - E_{path}}\right),$$

where

$$E_{path} = \frac{2}{N(N-1)} \sum_{i=1}^{N-1} \frac{N-i}{i}.$$

Graph Index Complexity (*Cr*). The graph index complexity (*Cr*) was developed drawing upon the properties of the largest eigenvalue of the adjacency matrix, the index r. This index has a maximum value of $2 \cdot \cos\frac{\pi}{N+1}$ for a clique, and a minimum value of $N-1$ for a path. Therefore, this heuristic graph complexity measure can be calculated as:

$$Cr = 4c_r(1 - c_r),$$

where

$$c_r = \frac{r - 2 \cdot \cos\frac{\pi}{N+1}}{N - 1 - 2 \cdot \cos\frac{\pi}{N+1}},$$

and $0 \leq Cr \leq 1$.

Entropy Measures

Offdiagonal Complexity (*OdC*). The offdiagonal complexity (*OdC*) measures the diversity in the node-node link correlation matrix $\{c_{ij}\}$ (Claussen 2007). This matrix computes the number of all neighbors with degree $j \geq i$ of all nodes with degree i. *OdC* is high for a network where the nodes of a given degree have no preference for the degree of their neighbors. *OdC* is zero for regular or fully connected networks, low for random networks and high for scale-free and hierarchical networks. The normalized version of *OdC* ($0 \leq OdC \leq 1$) is:

$$OdC = -\frac{\sum_{N=0}^{k_{max}-1} \tilde{a}_N \cdot \log \tilde{a}_N}{\log(N-1)},$$

where

$$\tilde{a}_N = a_N / \sum_{N=0}^{k_{max}-1} a_N.$$

Spanning Tree Sensitivity (*STS*). The spanning tree sensitivity (*STS*) is based on the idea that complex graphs should have diverse edge sensitivities. For each edge from node *i* to node *j* sensitivity is defined as:

s_{ij} = number of spanning trees of the graph - number of spanning trees of the corresponding one-edge-deleted subgraph

STS complexity is calculated as:

$$STS = H(S_{ij})/\log m_{cu},$$

where

$$H(\{S_{ij}\}) = -\sum_{l} a_l \cdot \log a_l, \quad a_l = S_{ij}^{l} / \sum_{r}^{k} S_{ij}^{r},$$

and

$$S_{ij} = s_{ij} - (\min s_{ij} - 1).$$

Spanning Tree Sensitivity Differences (*STSD*). The spanning tree sensitivity differences (*STSD*) is defined, similarly to *STS*, as:

$$STSD = H(Ld)/\log(m_{cu} - 1),$$

and is $0 \leq STSD < 1$. The difference is that first it is constructed an ordered list of the *k* different sensitivities, and then another list containing their differences, such as:

$$L = \{S_{ij}^{2} - S_{ij}^{1}, \ldots, S_{ij}^{k} - S_{ij}^{k-1}\}.$$

Subgraph Measures

One-Edge-Deleted Subgraph Complexity with Respect to the Different Number of Spanning Trees ($C_{1e,ST}$) *and One-Edge-Deleted Subgraph Complexity with Respect to the Different Spectra of the Laplacian Matrix* ($C_{1e,spec}$). These complexity measures are based on the idea that the more different subgraphs a graph contains, the more complex it is. In this manner, it is computed the *m* subgraphs resulting from the deletion of one edge. There are basically two forms of determining if two networks with the same number of nodes and edges are equivalent: a) if they have the same number of spanning trees, b) if they have the same spectrum of the Laplacian matrix. These two criteria give rise to two different complexity measures ($0 \leq C_{ie} < 1$):

$$C_{1e,ST} = (N_{1e,ST} - 1)/(m_{cu} - 1),$$

where $N_{1e,ST}$ is the number of different subgraphs, according to the different number of spanning trees, after cutting one edge.

$$C_{1e,spec} = (N_{1e,spec} - 1)/(m_{cu} - 1),$$

where $N_{1e,spec}$ is the number of different subgraphs, according to different spectra of the Laplacian and the signless Laplacian matrix, after cutting one edge.

Topological Descriptors

Distance-Based Descriptors

Wiener Index. The Wiener index, called it initially path number, was the first topological descriptor devised. It represents the sum of the distances between any two nodes in the network. It can be calculated by multiplying the number of nodes on one side of any edge by those on the other side, and adding all theses values for all edges (Wiener 1947).

Balaban J Index. The distance matrix (DM) is richer in information than the adjacency matrix (AM). The distance sum (DS) for each node is obtained by the addition of the row or column of the DM corresponding to that node. Thus, distance sums (s_j) are comparable to node degrees, which are obtained by the same addition in the AM. Consequently, they are often called distance degrees. Average distance sums ($\bar{s}_j$) result when dividing distance sums by the number of edges (q). In this manner, the Balaban J index, or average distance sum connectivity, is calculated (Balaban 1982). *J* increases with increasing branching.

Compactness. The average or mean distance between nodes in a network is a natural measure of its compactness (Doyle and Graver 1977).

Centralization. Centralization or distance graph deviation was calculated (Skorobogatov and Dobrynin 1988).

Other-Invariants Descriptors

Zagreb Index. The Zagreb index (Z_2) was computed (Nikolić et al. 2003).

Randić Connectivity Index. The Randić index, or connectivity index, is analogous to the Balaban J index (in fact, the latter was inspired by the former), but with node degrees instead of distance degrees (Randić 1975).

Complexity Index B. The complexity index B is based on the local invariant $b_i = k_i/s_i$, where k_i is the node degree and s_i is the distance degree (Bonchev and Rouvray 2005).

Normalized Edge Complexity. The normalized edge complexity, or connectedness, is defined as the ratio between the global edge complexity, the sum of all node degrees, and the number of edges in the complete graph (Bonchev and Rouvray 2005).

Entropy-Based Descriptors

Topological Information Content. The topological information content was first developed by Rashevsky with the idea of developing a complexity measure of graphs,

based on the number of different, distinguishable units of a network. If the network is composed of indistinguishable units, then its information content is 0. If the network is composed of N distinguishable units with equal probability, then its information content is $\log N$ (Rashevsky 1955; Mowshowitz 1968).

Bonchev Index. The Bonchev index I_W (Bonchev and Trinajstić 1977), or information index on the magnitude of distances, represents the information on the partitioning the Wiener index into groups of distances of the same magnitude.

Bertz Complexity Index. The Bertz complexity index was calculated (Bertz 1981).

Radial Centric Information Index. The radial centric information index was computed (Bonchev 1983).

Balaban-Like Information Indices. The Balaban-like information indices U and X were calculated (Balaban and Balaban 1991).

Edge Equality. A probability can be constructed for the edges of the network by partitioning them into g subsets depending on the equality of their partial connectivity indices. An information index on the edges distribution in the network according to their equivalence (Bonchev et al. 1981) can then be calculated.

Information Layer Index. The information layer index of a network was computed (Konstantinova et al. 2003).

Eigenvalue-Based Descriptors

Estrada and Laplacian Estrada Indices. The Estrada (EE) and Laplacian Estrada (LEE) indices were calculated (Mueller et al. 2014).

Energy and Laplacian Energy Indices. The energy (E) and Laplacian energy (LE) of a network were computed (Gutman and Zhou 2006).

Core Size

A core consists of a group of central and densely interconnected high-degree nodes which governs the overall behavior of a network, such as adaptability, flexibility and controllability (Ma and Mondragón 2015). A large core makes a network more flexible and adaptable to changes, whereas a small core makes a network more controllable. Nodes are ranked according to their degree in descending order. Their links are then divided into two groups: connections to nodes of higher rank (k_r^+) and lower rank ($k_r - k_r^+$). A node with few links with higher ranked nodes is probably at the periphery, that is, outside the core. Starting from the highest ranked node, the limit of the core is established at the node where k_r^+ reaches its maximum. The relative core size (c) is the ratio between the number of nodes in the core and the total number of nodes of the network.

Error and Attack Tolerance of Complex Networks

Many complex systems display a high degree of tolerance against errors. This robustness is often attributed to the redundant wiring of the network's elements. However, error tolerance comes at a high price: these networks are extremely vulnerable to attacks (Albert et al. 2000). This behavior can be simulated and tested by the random (error) or selected (attack) removal of nodes, and assessment of the resultant loss of connectivity. Three different attack strategies were evaluated: betweenness-based attack, degree-based attack and cascading attack, where betweenness is recalculated after each node is removed.

Software

Network analysis was carried out using the R programming language (R Development Core Team 2012; Ihaka and Gentleman 1996). Various packages from this project were used for different purposes. The package *igraph* (Csárdi and Nepusz 2006) was used for network parameter and modularity analysis. The package *brainGraph* (Watson 2017) was used for ZP space analysis and the package *WGCNA* (Langfelder and Horvath 2008) for Topological Overlap analysis. The package *QuACN* (Mueller et al. 2011) was used for complexity analysis. The package *NetSwan* (Lhomme 2015) was used for network strengths and weaknesses analysis. Visual network analysis was carried out using the program *Gephi* (Bastian et al. 2009).

Results

Description and Analysis of Networks

The majority of the groups belonging to the superorder Eucarida, class Malacostraca, were modeled as networks. These groups, ordered in evolutionary sequence, were the following: Euphausiacea, Dendrobranchiata, Caridea, Astacidea, Palinura, Anomura and Brachyura. This order is congruent with the overall evolutionary trend found in the superorder, that is, from an elongate and cylindrical cephalothorax, and a well-developed and articulated abdomen (pleon), to a shortened and depressed cephalothorax, and a reduced and ventrally folded abdomen. This order is also supported by phylogenetic analysis (Dixon et al. 2003).

The most common network parameters are summarized in Fig. 1. All the measured parameters decreased, except for the density. The number of nodes and edges, and the

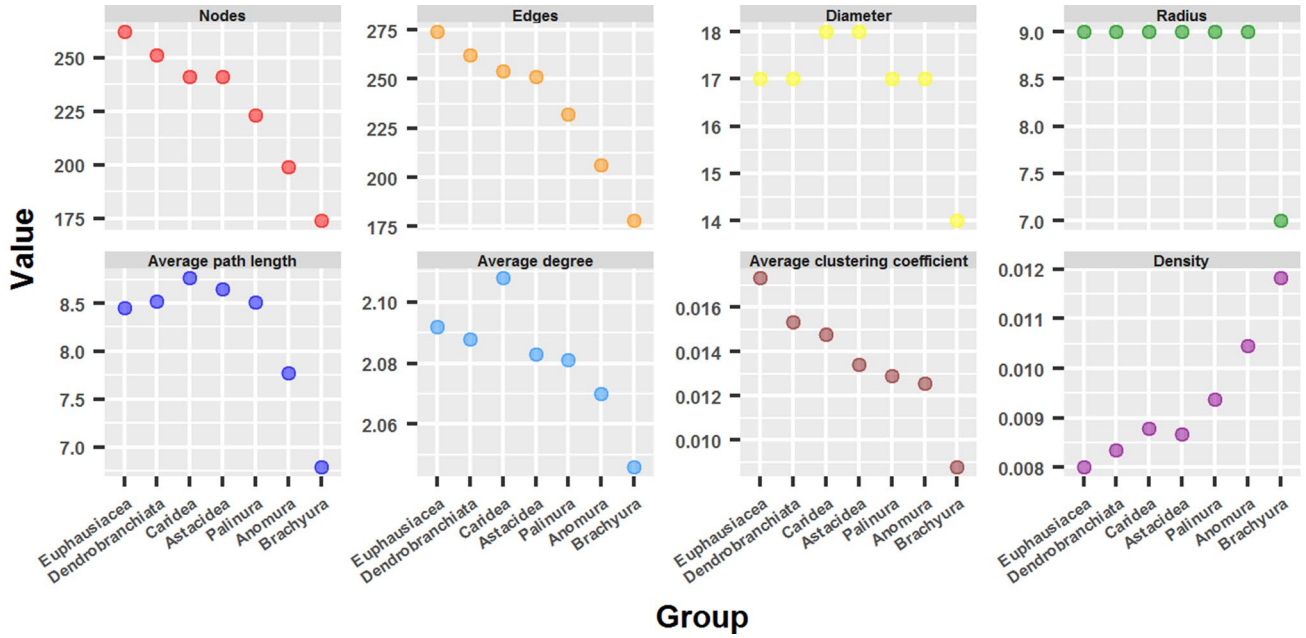

Fig. 1 Network parameters of the different stages of eucaridan evolution

average clustering coefficient decreased almost linearly. On the other hand, the diameter, radius, average path length and average degree decreased abruptly after a plateau phase that extended up to Palinura (average path length and average degree) or Anomura (diameter and radius). A mount or elevation could be observed in the aforementioned plateaus, except for the radius where the plateau was completely flat. The network density increased exponentially, so that the slope of the curve became steeper from the Astacidea group onwards.

According to these results, the evolution of the superorder is then characterized by a an important decrease in the size of the network: 33.6% of the nodes were lost from Euphausiacea to Brachyura. A similar decrease was observed in the number of edges (35%). The distance parameters, such as average path length (19.6%), diameter (17.65%) and radius (22.2%), underwent a milder decrease. The decrease in average degree was very small (2.2%). On the other hand, the density suffered a major and considerable increase (47.7%).

Visual Analysis of Crab Evolutionary Networks

Networks corresponding to the different groups of the superorder Eucarida were studied with the software *Gephi* for visual analysis and comparison (Fig. 2). Node size is representative of their degree, whereas color is representative of their increasing betweenness centrality (from white to red) or closeness centrality (from blue to white). Size and color were scaled in all the networks in order to make comparisons possible.

The eucaridan networks are organized around a central node, that is, they are centralized networks. This central node corresponds to the carapace, and has a high degree and betweenness centrality. It reaches its highest value in the group Euphausiacea, in which its degree is 14 and its betweenness centrality is 24,254.5. This centrality of the node that corresponds to the carapace decreases and loses predominance with the evolution of the group, evidenced by a decrease in its node size and a turning of its node color to pink. Whereas the decrease in node degree occurred gradually, the fall in betweenness centrally, although occurring from the beginning, it happened especially from the Astacidea group onwards. Conversely, the drop in node degree and betweenness centrality seemed to be compensated by an increase in the node closeness centrality: the node corresponding to the carapace passed from a light blue color to white in the course of the evolution of the group. Again, this rise occurred and intensified from the Astacidea group onwards. This visual results were confirmed by an analytical analysis of these parameters. As can be seen in Fig. 3, not only the maximum betweenness centrality, which corresponds to the carapace (except for Brachyura), decreased, but also the mean betweenness centrality. As seen by visual analysis, the betweenness centrality decreased from the first group, Euphausiacea, but the fall becomes more pronounced from the Astacidea group onwards. This behavior was even more evident in the mean betweenness centrality, where the curve started at high values, it fell slowly at the beginning, and then dropped abruptly. On the other hand, the closeness centrality seemed to have an opposite behavior. It was

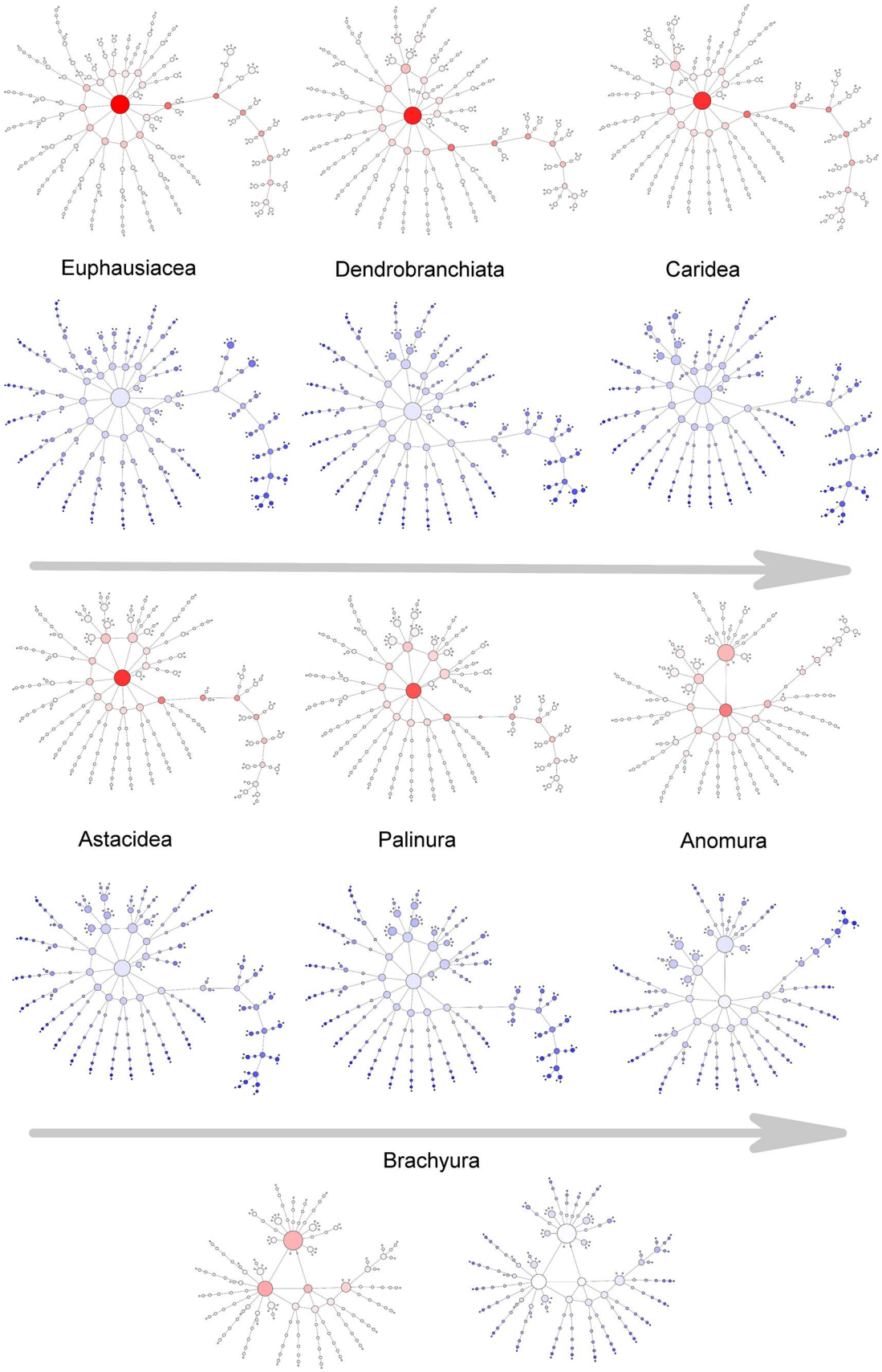

◂**Fig. 2** Eucaridan evolutionary networks. The networks corresponding to the different stages of eucaridan evolution were visually analyzed using *Gephi*. Networks were plotted using the Force Atlas layout algorithm. Node size corresponds to node degree, whereas node color corresponds to node betweenness centrality (from white to red) or closeness centrality (from blue to white). Networks were scaled so that comparisons can be made (Color figure online)

low and stable until the Astacidea group, and then it raised abruptly. This behavior was shared by both the mean and maximum closeness centrality. Therefore, the central node passes from possessing a high betweenness centrality to have a high closeness centrality. Moreover, this is true not only for the central node but for the overall network through the evolution of the superorder Eucarida.

Another interesting event through the evolution of the group was the change of the role and importance of the abdomen or pleon. It started with relatively high values of betweenness centrality in Euphausiacea, and then decreased gradually. Again, the fall in the values of betweenness centrality became more pronounced from the Astacidea group onwards, until Brachyura, where the presence and participation of the abdomen became almost negligible.

There was a substantial structural reorganization of the network in Brachyura. The node corresponding to the carapace lost predominance, evidenced by an important decrease in node degree and betweenness centrality, and led to an organization where a node trinity seemed to gain prevalence. This node trinity was composed of the nodes corresponding to the cephalon (7044), the fused thoracomere 1–4 (8238.5) and the carapace (6302.5). This core concentrated a high betweenness centrality (individual values in parentheses). However, it was distributed in three different nodes. These results were confirmed and expanded in this work by the evidence that this triadic structure appears as a high closeness centrality core, as can be seen in Fig. 2, where these three nodes appear as the whitest nodes of the entire evolutionary network series. These nodes form a core that is structurally enclosed and buried within the network, producing a kind of topological closure.

In this context, the Anomuran network seemed to be an intermediate or transition case. The structure of this network seemed to consist of a quasi-dyadic core, formed by the carapace (12,302) and the cephalon (6715), which concentrated a relatively high betweenness centrality (in parentheses). At the same time, both nodes had intermediate values of closeness centrality (around 0.0012). However, this dyadic structure was not enough to generate the topological closure observed in Brachyura, and the network's topology was still open.

Finally, the Palinuran network marked the beginning and starting point of the metamorphosis. Its overall structure was similar to its predecessors, that is, it was organized around a unique central node. However, the betweenness centrality of this node (16,266) has already dropped 32.9% and it was halfway between the extreme values of Euphausiacea and Brachyura. On the other hand, it has already gained higher values of closeness centrality, both in maximum and mean values, confirming the initiation of the structural reorganization.

The Passage from Betweenness Centrality to Closeness Centrality

We have seen in Fig. 3 that the evolution of the superorder Eucarida was characterized by a decrease in betweenness centrality and an increase in closeness centrality. In order to study this in more detail, the nodes' betweenness versus closeness centrality were plotted (Fig. 4). This analysis showed that with the evolution of the group, the successive point clouds acquired a steeper slope, which resulted in higher closeness centrality values, at the expense of the lowering of their betweenness centrality. The first four groups (Euphausiacea, Dendrobranchiata, Caridea and Astacidea) were nearly indistinguishable, except for Euphausiacea which had a bit lower slope than the other three. However, the first group that gave a clearly distinguishable point cloud separated from the basal behavior was the Palinuran network, which departed from the first four groups at a betweenness centrality of approximately 7000. The Anomuran network departed from the first four groups at a betweenness centrality of approximately 3500, but with a steeper slope and reaching substantially higher values of closeness centrality. Finally, the Brachyuran network departed from the first four groups at a betweenness centrality of approximately 700 and had the steepest slope and the highest values of closeness centrality. Therefore, it was certain to affirm that there was a transformation and a passage from betweenness centrality to closeness centrality in the networks representing the evolution of Eucarida.

The most important result obtained with this analysis was that it was possible to trace the identity and evolution of the central node. In the first six groups, this central node consisted of a unique node with the highest betweenness and closeness centrality. It could be observed that with the evolution of the group, this central node moved diagonally from a zone of high betweenness centrality (and low closeness centrality) to a zone of high closeness centrality (and low betweenness centrality). Surprisingly, in Brachyura, in the zone where the central node was expected to appear, three nodes appeared instead. These three nodes corresponded to the triadic structure (cephalon, thoracomere 1–4 and carapace) detected and analyzed in the previous section. Therefore, this evidence supported the results and conclusions arrived at that section.

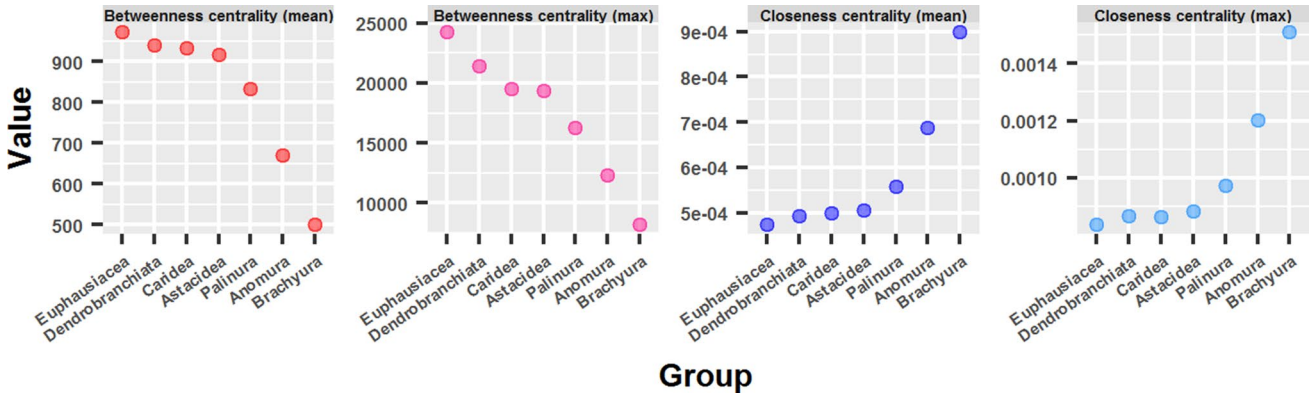

Fig. 3 Variation of betweenness centrality and closeness centrality, mean and maximum, during eucaridan evolution (Color figure online)

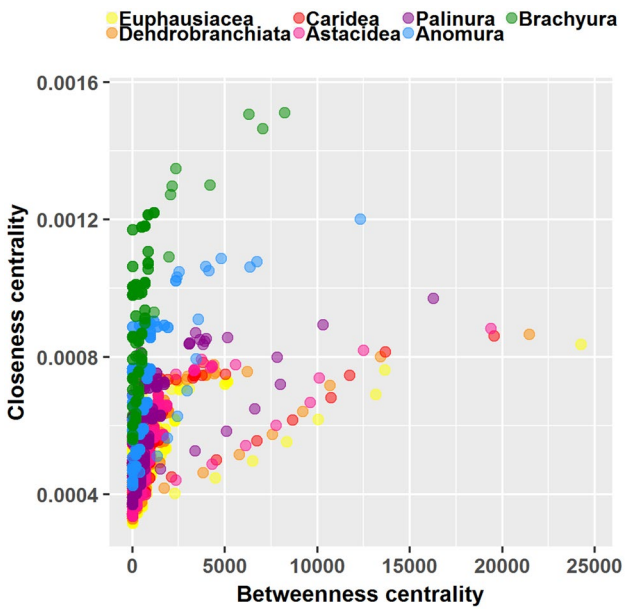

Fig. 4 Betweenness centrality vs. closeness centrality during eucaridan evolution. There is a shift from a zone of high betweenness centrality to a zone of high closeness centrality. It can be seen that the outperformer node follows this behavior, forming an exponential curve, and passes from a single node throughout evolution to a node trinity in the last stage of evolution (Brachyura)

Modularity

The method used for module detection and identification was multi-level optimization of modularity (Blondel et al. 2008). The networks representing crab evolution resulted to be highly modular. Modularity slightly decreased during evolution from 0.837 in Euphausiacea to 0.802 in Brachyura, that is, a 4.18% reduction (Fig. 5). On the other hand, the number of communities increased gradually during evolution from 27 in Euphausiacea to 30 in Astacidea and Palinura, and decreased abruptly to 24 in Brachyura.

The structure and membership of the modules identified in each network is visualized and summarized in Fig. 6 and Tables 1, 2, 3, 4, 5, 6 and 7. In general terms, each appendage was defined as a singular module. There were some exceptions to this rule, especially in those cases where the appendages consisted of few nodes. In these cases, these appendages were part of larger adjacent modules, in general the modules including the body segments. These segments formed more complex modules that varied their membership and structure during evolution.

In Euphausiacea (Fig. 6a and Table 1), all the head and thoracic segments, plus the carapace, eyes, seventh and eighth thoracopods, formed the module 3. This determined no modular separation between the head and thorax. On the other hand, the abdomen (pleon) was formed by 4 axially arranged modules (24, 25, 26 and 27). In Dendrobranchiata (Fig. 6b and Table 2), the same general modular arrangement was found. Module 3 concentrated all the head and thoracic segments, the carapace, eyes and mandibles. The fusion of head segment 6 with thoracomere 1 occurred at this stage. On the other hand, the abdomen, in this case, was divided in 3 modules (26, 27 and 28). In Caridea (Fig. 6c and Table 3), a similar pattern was also found. Module 3 contained all the head and thoracic segments, the carapace, eyes and maxillule. On the other hand, the abdomen was composed of three axially arranged modules (26, 28 and 29), whereas the left third pleopod formed its own individual module (27). In Astacidea (Fig. 6d and Table 4), module 3 was formed by all the head and thoracic segments, the carapace and eyes. In this group, the fusion of head segment 4 and 5 was detected. The abdomen was composed of three modules (28, 29 and 30). In Palinura (Fig. 6e and Table 5), the head and thoracic segments, carapace and eyes were contained in module 13. The fusion of head segment 2 and 3 occurred at this stage of evolution. Meanwhile, the

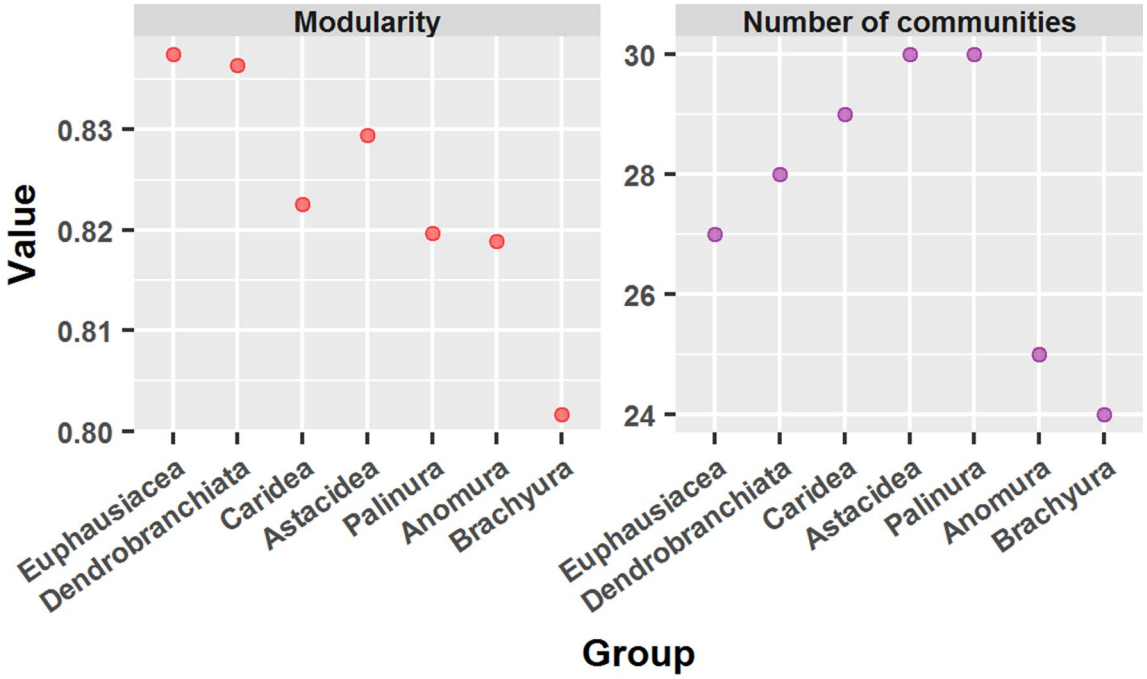

Fig. 5 Modularity and number of communities in the networks corresponding to the different stages of eucaridan evolution, obtained by multilevel optimization of modularity

abdomen was composed of 3 axially arranged modules (28, 29 and 30). In Anomoura (Fig. 6f and Table 6), the general modular plan and pattern seen up to now suffered an abrupt and drastic structural modification. The head and thoracic segments, which were contained in a single module from Euphausiacea to Palinura, became part of different modules. This seemed to be triggered by the complete fusion of head segments 1–5, forming what has been called the cephalon. In this manner, module 1 was composed of the cephalon, eyes, right antennula, mandibles and maxillule; whereas module 9 was made up by the thoracic segments, the carapace and right second maxilliped (protopod and exopod). On the other hand, the abdomen suffered a reduction and became to be formed by only two modules (24 and 25). Finally, in Brachyura (Fig. 6g and Table 7), the fusion of thoracomeres 1–4 further endorsed the tendency and structural reorganization initiated in Anomura. Now, module 5 contained the cephalon (which became to be formed by the fusion of head segments 1–6), eyes, right mandible, maxillule and maxillae; whereas module 13 was made up by the thoracic segments, the carapace and penes. On the other hand, the abdomen continued its reduction and became to be formed by only one module (24).

In consequence, during evolution the group suffered a division of the body in two modules, which could be regarded as the head and thorax tagmata, and a reduction of the abdomen (pleon), which started having four modules and ended up having only one module. This modular delimitation of tagmata, in which each tagma (head, thorax and abdomen) was represented and defined by a single axial module, was accomplished in the last stage of eucaridan evolution, that is, in Brachyura.

Finally, the inspection of the networks depicted in Fig. 6, plotted using the Fruchterman-Reingold layout algorithm, it was possible to discern, in the region corresponding to the body, the passage from a monadic (in Euphausiacea, Dendrobranchiata, Caridea, Astacidea and Palinura), to a dyadic (in Anomura), and finally to a triadic structure (in Brachyura). In the first case, all the appendages protruded radially from a single center. In the second case, the anterior and posterior appendages protruded from two different centers and headed to opposite directions (180°). In the third case, the anterior, intermediate and posterior appendages protruded from three different centers and headed to three directions as the corners of a triangle (120°).

ZP Space: Node Roles Within a Module

In order to characterize the role of each node within its corresponding module, I performed a ZP space analysis (Guimera and Amaral 2005) to all the networks of the crab evolutionary series.

In general terms, nodes with high values of z have high within-module degree, that is, they are nodes with many intramodular connections and, therefore, they are considered module hubs. On the other hand, nodes with

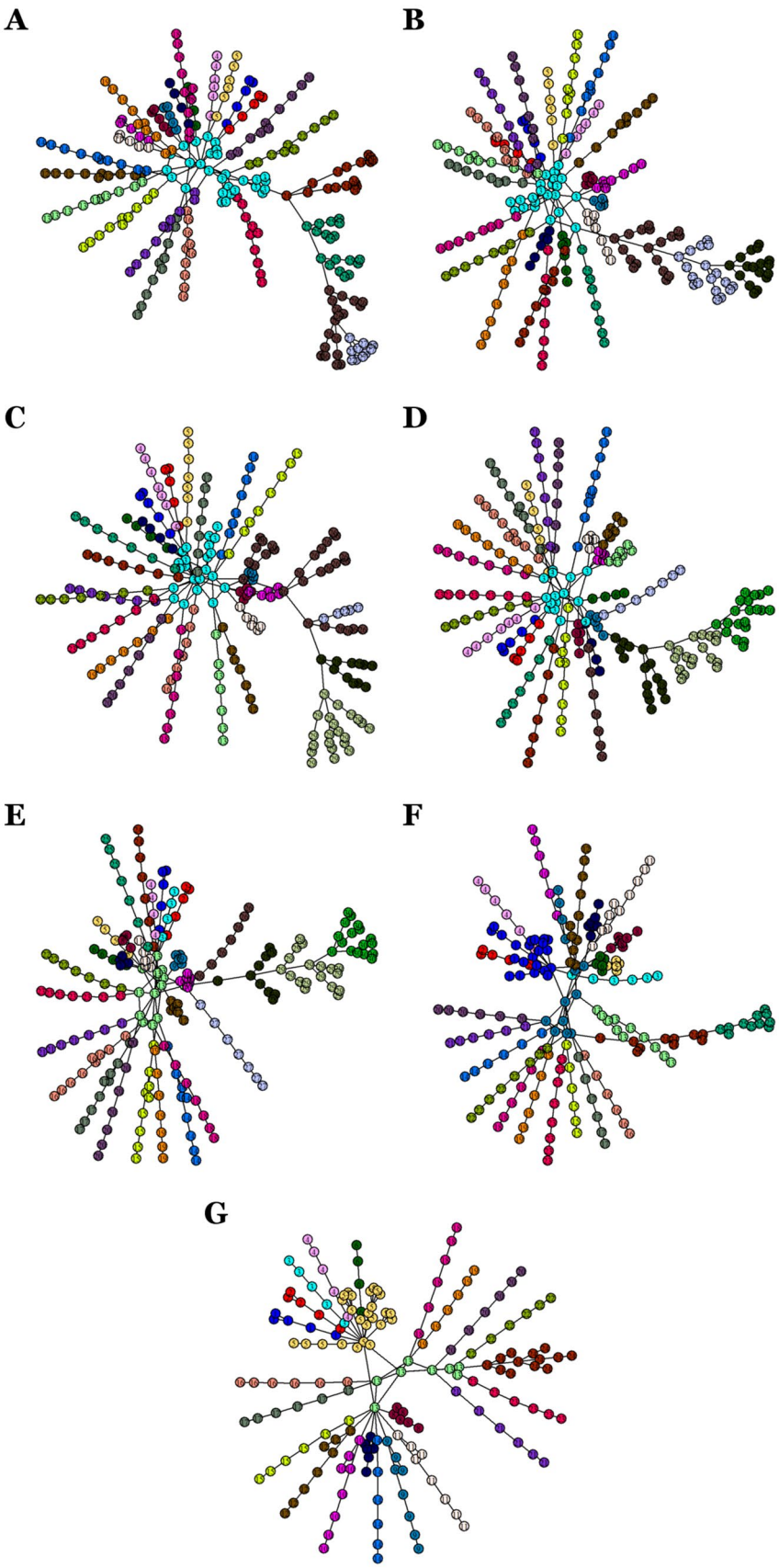

Fig. 6 Detection and identification of modules in the evolutionary network series: **a** Euphausiacea, **b** Dendrobranchiata, **c** Caridea, **d** Astacidea, **e** Palinura, **f** Anomura, **g** Brachyura. Modules, obtained by multi-level optimization of modularity, are identified with different numbers and colors in the figure, and their composition detailed and specified in the accompanying table. Networks were plotted using the Fruchterman–Reingold layout algorithm (Color figure online)

Table 1 Modules in the network corresponding to Euphausiacea

Module	Membership
1	Right antennula
2	Left antennula
3	Carapace, head segment 1–6, eyes, thoracomere 1–8, seventh thoracopods, eighth thoracopods
4	Right antenna
5	Left antenna
6	Right mandible
7	Left mandible
8	Right maxillula
9	Left maxillula
10	Right maxilla
11	Left maxilla
12	Right first thoracopod
13	Left first thoracopod
14	Right second thoracopod
15	Left second thoracopod
16	Right third thoracopod
17	Left third thoracopod
18	Right fourth thoracopod
19	Left fourth thoracopod
20	Right fifth thoracopod
21	Left fifth thoracopod
22	Right sixth thoracopod
23	Left sixth thoracopod
24	Pleomere 1, first pleopods
25	Pleomere 2 and 3, second pleopods, third pleopods
26	Pleomere 4 and 5, fourth pleopods, fifth pleopods
27	Pleomere 6, uropods, telson, lateral processes

Table 2 Modules in the network corresponding to Dendrobranchiata

Module	Membership
1	Right antennula
2	Left antennula
3	Carapace, head segment 1–3, eyes, gnathothoracomere 1–11 (3-4 fused), mandibles
4	Right antenna
5	Left antenna
6	Right maxillula
7	Left maxillula
8	Right maxilla
9	Left maxilla
10	Right first maxilliped
11	Left first maxilliped
12	Right second maxilliped
13	Left second maxilliped
14	Right third maxilliped
15	Left third maxilliped
16	Right first pereopod
17	Left first pereopod
18	Right second pereopod
19	Left second pereopod
20	Right third pereopod
21	Left third pereopod
22	Right fourth pereopod
23	Left fourth pereopod
24	Right fifth pereopod
25	Left fifth pereopod
26	Pleomere 1 and 2, first pleopods, second pleopods
27	Pleomere 3 and 4, third pleopods, fourth pleopods
28	Pleomere 5 and 6, fifth pleopods, uropods, telson

high participation coefficient are nodes with many intermodular connections, their connections are distributed among different modules and, therefore, they are considered connectors. The ZP space was divided in 7 regions, each one corresponding to a different role. Nodes with $z \geq 1$ were considered hubs, whereas nodes with $z < 1$ were regarded as non-hubs. Hubs with $z \geq 2.75$ were considered super-hubs. Nodes with $P \geq 0.4$ were classified as connectors, whereas nodes with $P < 0.4$ were classified as non-connectors. Connectors with $P \geq 0.75$ were classified as hyper-connectors. In this manner, the 7 identified regions were the following: peripheral nodes, i.e. nodes with most or all their links within their module (lightblue region, $z < 1$ and $P < 0.4$); non-hub connector nodes, i.e. nodes with many links to other modules (yellow region, $z < 1$ and $0.4 \leq P < 0.75$); non-hub hyper-connectors nodes, i.e. nodes with most of their links to other modules (green region, $z < 1$ and $P \geq 0.75$); local hubs, i.e. hub nodes with the majority of links within their module (pink region, $P < 0.4$ and $1 \leq z < 2.75$); local super-hubs, i.e. super-hubs with the majority of links within their module (violet region, $P < 0.4$ and $z \geq 2.75$); connector hubs, i.e. hubs with many or most of their links to other modules (orange region, $P \geq 0.4$ and $1 \leq z < 2.75$); and connector super-hubs, i.e. super-hubs with many or most of their links to other modules (red region, $P \geq 0.4$ and $z \geq 2.75$).

In the Euphausiacea network, 72.14% of nodes were peripheral nodes (Fig. 7a). The rest of the nodes were non-hub connectors (12.98%) or local hubs (14.5%). The most distinctive characteristic of this network was the presence of a local super-hub (violet region), represented by the carapace. This node had a high within-module degree (4.587) and an almost null participation coefficient. The within-module degree achieved by the local super-hub in Euphausiacea was the highest obtained in the whole evolutionary series.

In the Dendrobranchiata network, a similar percentage of peripheral nodes was found (71.31%) (Fig. 7b). However, an increase in local hubs was detected (16.73%) at the expense of a decrease in non-hub connectors (11.55%). The node

Table 3 Modules in the network corresponding to Caridea

Module	Membership
1	Right antennula
2	Left antennula
3	Carapace, head segment 1–5, eyes, maxillule, thoracomere 1–8 (1 fused to head segment 6)
4	Right antenna
5	Left antenna
6	Right mandible
7	Left mandible
8	Right maxilla
9	Left maxilla
10	Right first maxilliped
11	Left first maxilliped
12	Right second maxilliped
13	Left second maxilliped
14	Right third maxilliped
15	Left third maxilliped
16	Right first pereopod
17	Left first pereopod
18	Right second pereopod
19	Left second pereopod
20	Right third pereopod
21	Left third pereopod
22	Right fourth pereopod
23	Left fourth pereopod
24	Right fifth pereopod
25	Left fifth pereopod
26	Pleomere 1–3, first pleopods, second pleopods, right third pleopod
27	Left third pleopod
28	Pleomere 4, fourth pleopods
29	Pleomere 5 and 6, fifth pleopods, uropods, telson

corresponding to the carapace was still categorized as a local super-hub, although a decrease in the within-module degree was registered (4.082). In this case, the participation coefficient of this node was zero.

In Caridea, a similar percentage of peripheral nodes was also found (72.2%) (Fig. 7c). However, it was registered an inversion in the percentages between local hubs and non-hub connectors. Contrary to the previous cases, the percentage of non-hub connnectors (14.94%) was superior to the percentage of local hubs (12.45%). The situation of the node corresponding to the carapace was identical to the previous case, that is, it had the same values of within-module degree and participation coefficient.

In Astacidea, a slight increase in the percentage of peripheral nodes was registered (74.27%) (Fig. 7d). This happened at the expense of a decrease in the percentage of non-hub connectors (12.86%), falling to a similar value to the one found in local hubs (12.45%). The node corresponding to the carapace was still detected as a local super-hub, as well as a further decrease in the within-module degree (3.431). No change in its participation coefficient was detected.

In the Palinura network, a slight decrease in the percentage of peripheral nodes was registered (73.54%) (Fig. 7e). This was accompanied by an increase in the percentage of non-hub connectors (13.9%). The percentage of local hubs remained at similar values (12.11%). The downward trend in the within-module degree in the node corresponding to the carapace continued (3.259), as well as its null participation coefficient and its categorization as a local super-hub.

In Anomura, the accumulated changes during the previous stages of evolution bursted and produced radical changes in the network structure. Firstly, it occurred an increase in the percentage of peripheral nodes (79.4%), accompanied by a decrease in the percentage of non-hub connectors (11.56%) and especially local hubs (7.54%) (Fig. 7f). Most importantly, two unique novelties appeared in this network. In the first place, it was detected the presence of a non-hub hyper-connector (green region),

Table 4 Modules in the network corresponding to Astacidea

Module	Membership
1	Right antennula
2	Left antennula
3	Carapace, head segment 1–5 (4–5 fused), eyes, thoracomere 1–8 (1 fused to head segment 6)
4	Right antenna
5	Left antenna
6	Right mandible
7	Left mandible
8	Right maxillula
9	Left maxillula
10	Right maxilla
11	Left maxilla
12	Right first maxilliped
13	Left first maxilliped
14	Right second maxilliped
15	Left second maxilliped
16	Right third maxilliped
17	Left third maxilliped
18	Right first pereopod
19	Left first pereopod
20	Right second pereopod
21	Left second pereopod
22	Right third pereopod
23	Left third pereopod
24	Right fourth pereopod
25	Left fourth pereopod
26	Right fifth pereopod
27	Left fifth pereopod
28	Pleomere 1 and 2, first pleopods, second pleopods
29	Pleomere 3 and 4, third pleopods, fourth pleopods
30	Pleomere 5 and 6, fifth pleopods, uropods, telson

Table 5 Modules in the network corresponding to Palinura

Module	Membership
1	Right antennula
2	Left antennula
3	Right antenna
4	Left antenna
5	Right mandible
6	Left mandible
7	Right maxillula
8	Left maxillula
9	Right maxilla
10	Left maxilla
11	Right first maxilliped
12	Left first maxilliped
13	Carapace, head segment 1, head segment 2–3 (fused), head segment 4-5 (fused), eyes, thoracomere 1–8 (1 fused to head segment 6)
14	Right second maxilliped
15	Left second maxilliped
16	Right third maxilliped
17	Left third maxilliped
18	Right first pereopod
19	Left first pereopod
20	Right second pereopod
21	Left second pereopod
22	Right third pereopod
23	Left third pereopod
24	Right fourth pereopod
25	Left fourth pereopod
26	Right fifth pereopod
27	Left fifth pereopod
28	Pleomere 1 and 2, second pleopods
29	Pleomere 3 and 4, third pleopods, fourth pleopods
30	Pleomere 5 and 6, fifth pleopods, uropods, telson

represented by the thoracomere 1. In the second place, it was detected the presence of a connector super-hub (red region), represented by the cephalon. Both nodes had a high participation coefficient (0.816 and 0.611, respectively). The connector super-hub (cephalon) also had a high within-module degree (3.447). On the other hand, the carapace still was considered as a local super-hub, though its within-module degree fell to 2.976. Moreover, it was the first time that this node acquired an important participation coefficient (0.197).

Finally, in Brachyura, a similar percentage of peripheral nodes was found (79.31%) (Fig. 7g). Meanwhile, there was a slight increase in the percentage of non-hub connectors (13.22%), and a slight decrease in the percentage of local hubs (6.32%). The most important event at this stage of evolution was the complete disappearance of the carapace as a local super-hub (violet region). This node suffered a drastic reduction in the within-module degree (1.620), while it acquired an even higher participation coefficient (0.278). This resulted in the categorization of this node as a local hub. On the other hand, the non-hub hyper-connector and the connector super-hub were still present and represented, in this case, by the fused thoracomere 1–4 and the cephalon, respectively. Both nodes had a higher participation coefficient than the ones registered in Anomura (0.893 and 0.704, respectively), while the cephalon suffered a reduction in the within-module degree (3.021). The participation coefficient achieved by the non-hub hyper-connector in

Table 6 Modules in the network corresponding to Anomura

Module	Membership
1	Cephalon (head segment 1–5 fused), eyes, right antennula, mandibles, maxillule
2	Left antennula
3	Right antenna
4	Left antenna
5	Right maxilla
6	Left maxilla
7	Right first maxilliped
8	Left first maxilliped
9	Carapace, thoracomere 1–8 (1 fused to head segment 6), right second maxilliped (protopod and exopod)
10	Right second maxilliped (endopod)
11	Left second maxilliped
12	Right third maxilliped
13	Left third maxilliped
14	Right first pereopod
15	Left first pereopod
16	Right second pereopod
17	Left second pereopod
18	Right third pereopod
19	Left third pereopod
20	Right fourth pereopod
21	Left fourth pereopod
22	Right fifth pereopod
23	Left fifth pereopod
24	Pleomere 1–4, second pleopods, third pleopods, fourth pleopods
25	Pleomere 5 and 6, fifth pleopods, uropods, telson

Brachyura was the highest obtained in the whole evolutionary series.

Hierarchical Organization in Eucaridan Evolutionary Networks

In order to study the hierarchical organization of the eucaridan evolutionary network series, a topological overlap analysis was performed (Ravasz et al. 2002).

The results obtained with the topological overlap analysis showed that the networks possessed a hierarchical modular organization (Fig. 8). These networks presented two main characteristics: an evident modular organization and a module-within-module topological structure. This meant that the topological overlap matrix appeared with a series of clearly demarcated blocks of highly topological overlapping, some of which being part of even larger blocks, which is a clear evidence of hierarchical modular organization. Two basic types of hierarchical organization could be detected: local and global. The first one was detected and manifested by the module-within-module described above, which was always working at a short range. But another type of hierarchical organization was also detected and its main characteristic was the presence of a typical wing-like structure in the topological overlap matrix, which extended over long ranges. This basic pattern of hierarchical organization suffered different degrees of complexification along the evolutionary series as it will be explained below.

The topological overlap analysis revealed that the hierarchical organization of the networks increased during evolution. The topological overlap matrix corresponding to Euphausiacea showed a very simple pattern, characterized by the presence of a serially arranged group of blocks formed by module-within-module structures, i.e. local hierarchical organization (Fig. 8a). Two principal short wing-like structures were also detected, pointing to the presence of rather short-range global hierarchical organization. In Dendrobranchiata, the topological overlap matrix was similar than in the previous case, although three main short wing-like structures were present (Fig. 8b). In Caridea, the topological overlap matrix was quite different from the previous ones (Fig. 8c). For the first time, long-range global hierarchical organization was detected, evidenced by the appearance of a long wing-like structure. This matrix also showed the presence of 3 short and 1 medium wing-like structures. In Astacidea, the hierarchical organization seemed to return

Table 7 Modules in the network corresponding to Brachyura

Module	Membership
1	Right antennula
2	Left antennula
3	Right antenna
4	Left antenna
5	Cephalon (head segment 1–6 fused), eyes, right mandible, maxillule, maxillae
6	Left mandible
7	Right first maxilliped
8	Left first maxilliped
9	Right second maxilliped
10	Left second maxilliped
11	Right third maxilliped
12	Left third maxilliped
13	Carapace, thoracomere 1–4 (fused), thoracomeres 5–8, penes
14	Right first pereopod
15	Left first pereopod
16	Right second pereopod
17	Left second pereopod
18	Right third pereopod
19	Left third pereopod
20	Right fourth pereopod
21	Left fourth pereopod
22	Right fifth pereopod
23	Left fifth pereopod
24	Pleomere 1 and 2, pleomere 3–5 (fused), pleomere 6, first gonopods, second gonopods, telson

to a simpler pattern where only short and medium wing-like structures were apparent (Fig. 8d). In Palinura, the matrix appeared much more complex than the previous cases (Fig. 8e). One long and one medium wing-like structures were present forming a cross. Moreover, many short wing-like were dispersed and distributed among the blocks with module-within-module structures. In Anomura, the matrix became even more complex and added a new novelty (Fig. 8f). The long and medium wing-like structures forming a cross were still present, but a new structure appeared: a big block with module-within module structure. This type of hierarchical organization was not explained at the beginning of the section, and represented a combination of the other two types: it consisted of a block with module-within-module structure working at long ranges. Finally, in Brachyura, the topological overlap matrix was by far the most complex (Fig. 8g). Two long wing-like structures and at least three big blocks with module-within module structure were present. The pivotal roles in these structures were played by the cephalon, the fused thoracomere 1–4 and the carapace. Therefore, the network corresponding to Brachyura was the one with the highest hierarchical organization.

The associated hierarchical trees provided further evidence of our previous results. During evolution, the trees became more heterogeneous and their levels better demarcated, being distributed more clearly at different heights.

Complexity

Complexity Measures

The normalized complexity measures proposed by Kim and Wilhelm (2008) were tested on the eucaridan evolutionary network series.

The majority of the complexity measures increased during evolution (Fig. 9). In this manner, the medium articulation index (*MAg*) increased 27% from Euphausiacea to Brachyura, the efficiency complexity index (*Ce*) increased 18.35%, the graph index complexity (*Cr*) 25.1%, the offdiagonal complexity index (*OdC*) 23.9% and the one-edge-deleted subgraph complexity with respect to the spectra of the Laplacian matrix ($C_{1e,spec}$) 29.1%. In general terms, this complexity measures began to increase rapidly after a rather stable or lag phase that extended up to Astacidea (or Palinura in the case of *Ce*). On the other hand, the spanning tree sensitivity (*STS*) and the one-edge-deleted subgraph complexity with respect to the different number of spanning trees ($C_{1e,ST}$) decreased during evolution, 14.7% and 35.2%

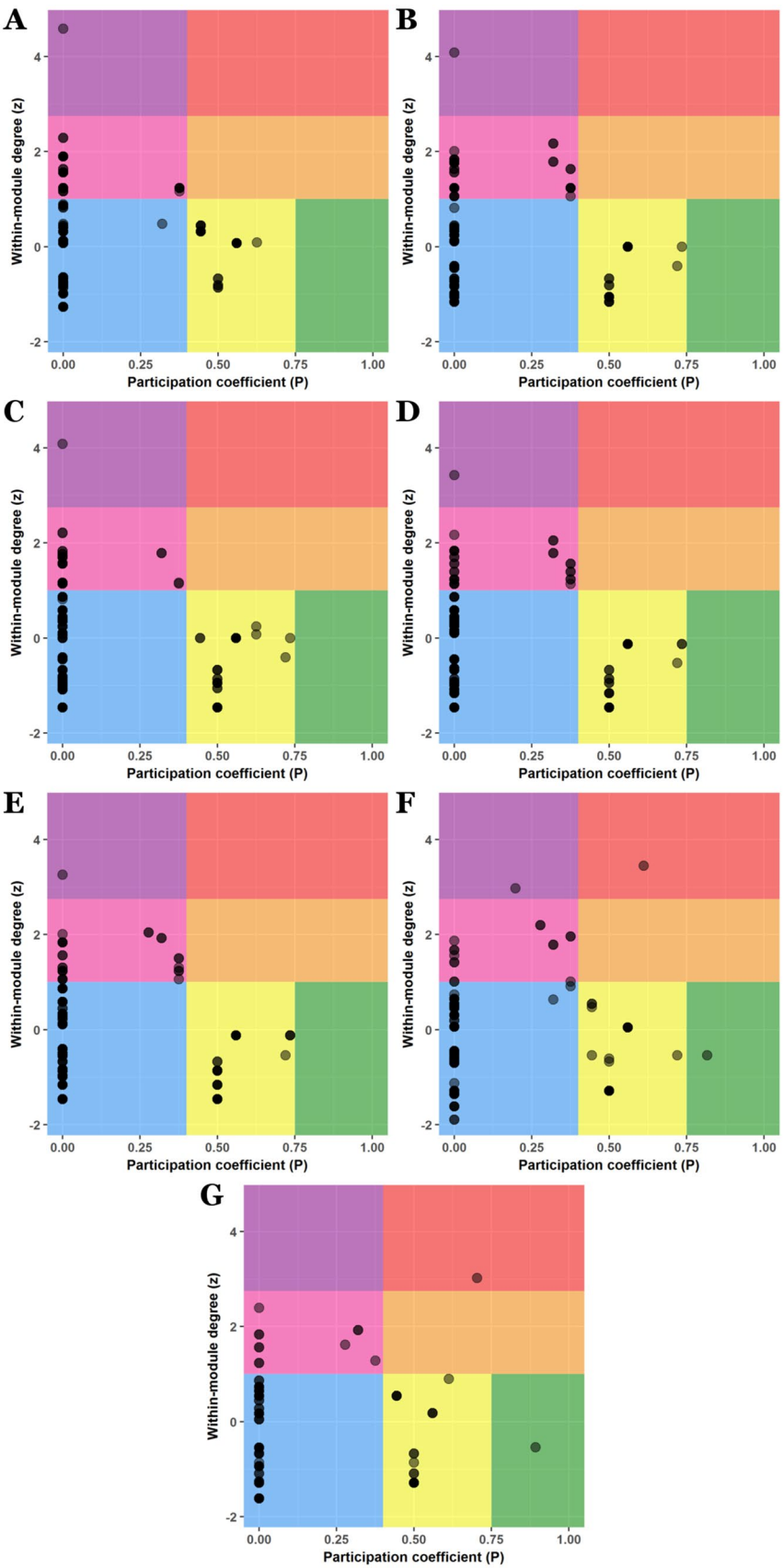

Fig. 7 ZP space analysis. **a** Euphausiacea, **b** Dendrobranchiata, **c** Caridea, **d** Astacidea, **e** Palinura, **f** Anomura, **g** Brachyura. See text for details and explanation of the different regions defined for the analysis

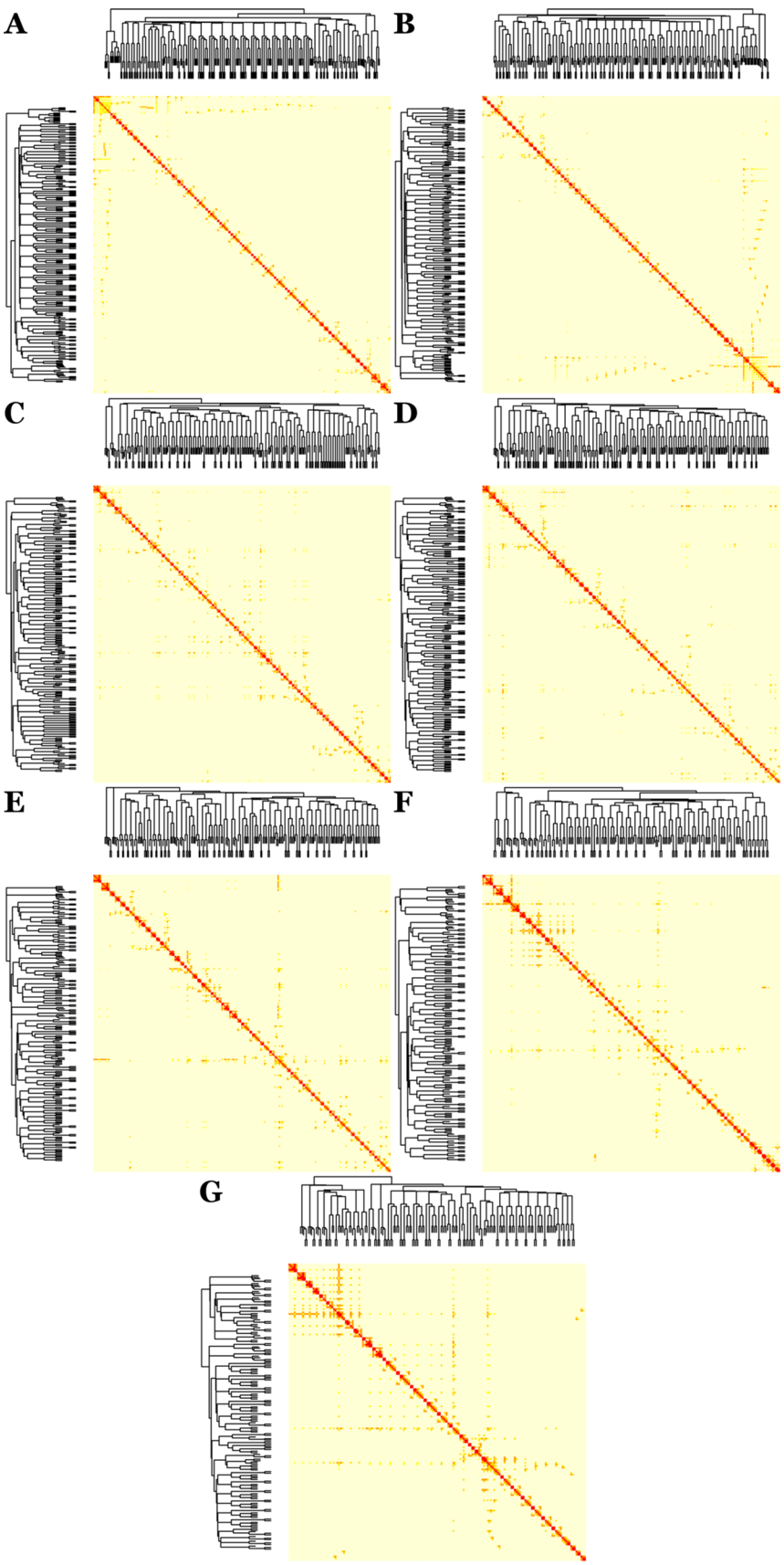

Fig. 8 Topological overlap analysis: hierarchical organization of eucaridan evolutionary networks. **a** Euphausiacea, **b** Dendrobranchiata, **c** Caridea, **d** Astacidea, **e** Palinura, **f** Anomura, **g** Brachyura. The heatmaps represents the different topological overlap matrices. Rows and columns correspond to individual nodes, light colors represent low topological overlap, whereas orange and red colors represent progressively higher topological overlap. The corresponding hierarchical trees are shown on the left and top (Color figure online)

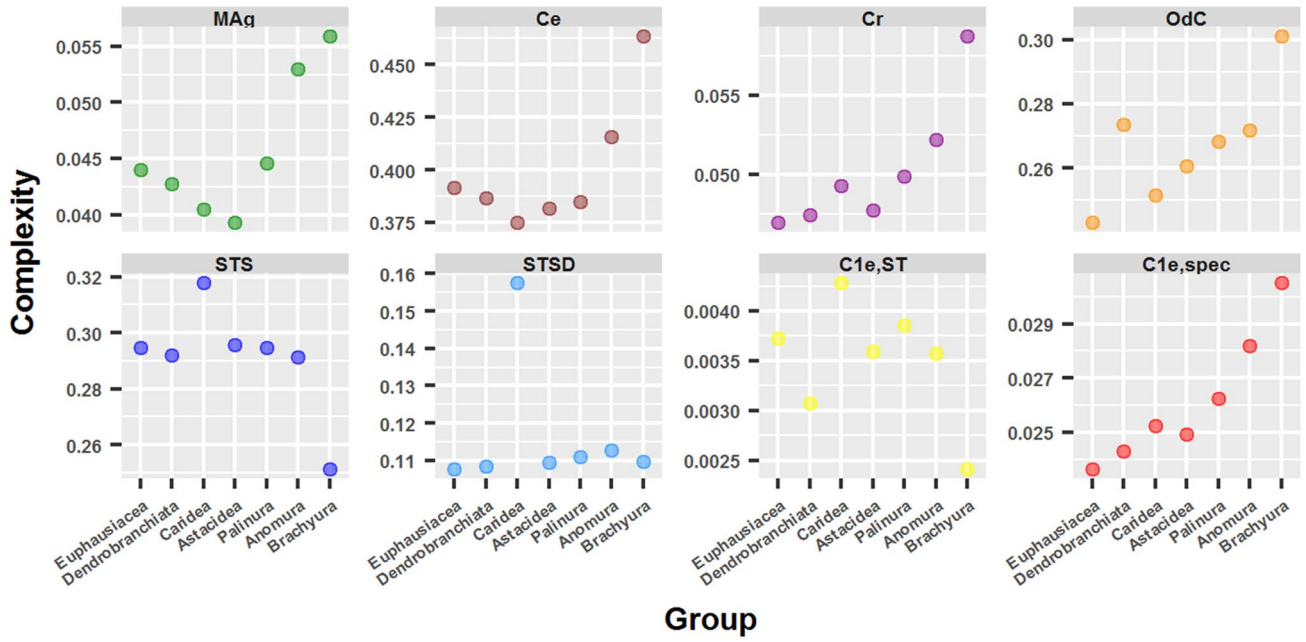

Fig. 9 Complexity measures: their variation during eucaridan evolution

respectively. In this case, the drop occurred at the passage from Anomura to Brachyura. Meanwhile, the spanning tree sensitivity differences (*STSD*) remained unchanged during evolution, except for a transitory increase in Caridea.

Topological Descriptors

Topological descriptors were tested on the eucaridan evolutionary network series. These descriptors are measures that enable the quantification of network structural information, their topology and metrical properties, and as such they behave as real structural complexity measures (Mueller et al. 2011, 2014; Dehmer et al. 2017).

Contrary to what happened with the previous complexity measures, the great majority of the topological descriptors decreased during evolution (Fig. 10). In general, this decrease became more pronounced at the stage corresponding to Astacidea (the overall percentage decrease is denoted in parentheses). Before that stage, the values decreased slower, such as in the Wiener index (64.6%), centralization (66.3%), Randić connectivity index (34.2%), Bonchev index (67.3%), Bertz complexity index (36.9%), graph distance complexity (7.5%), information theoretic complexity (7.6%), Estrada index (36%) and Laplacian energy (35.4%); or they even remained relatively stable, such as in the mean distance deviation (39.7%), compactness (19.6%), eccentricity (45.9%), average distance (46.7%), radial centric information index (10.7 %), graph vertex complexity index (9.9%), information layer index (40.5%) and energy (34.3%). Among the latter, the cases of compactness, radial centric information index and graph vertex complexity index stood out. They not only suffered a slight increase between Euphausiacea and Palinura, with their peak at Caridea, but their pronounced decrease started at a later stage (Palinura). On the other hand, the Harary index (45%), Zagreb index (27%) and spectral radius (10.4%) decreased almost linearly. Meanwhile, the topological information content (2%), edge equality (3.3%) and eigenvalue-based index (1.7%) showed a small decrease during evolution. The first one raised up to Caridea and then it decreased, reaching its minimum at Brachyura. The other two reported a sawed curve with an internal peak at Astacidea and a final rise in Brachyura.

Conversely, there were some topological descriptors that increased during evolution, as it was registered for the previous complexity measures (overall percentage increase in parentheses). These were the Balaban J index (87.6%), complexity index B (23.9%), normalized edge complexity (47.3%) and Balaban-like information index (107.1%). The Laplacian Estrada index (19.7%) could be included in this group, although it reported a singular behavior. It started at a high value in Euphausiacea, it decreased rather exponentially up to Palinura, when it reached its lowest value, and then it raised abruptly up to Brachyura, especially in the last stage from Anomura to Brachyura, reaching a final value higher than in Euphausiacea.

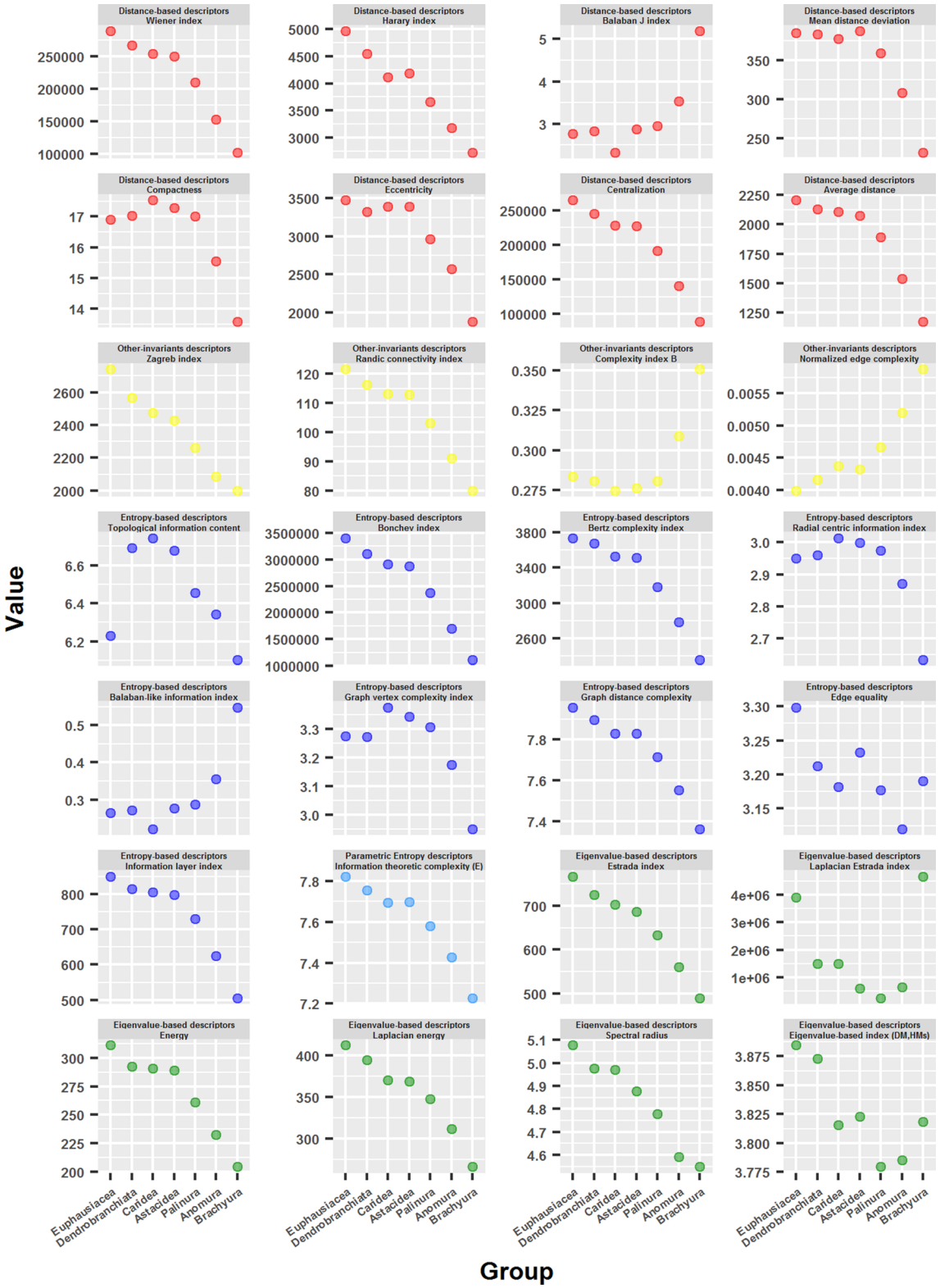

Fig. 10 Topological descriptors: their variation during eucaridan evolution

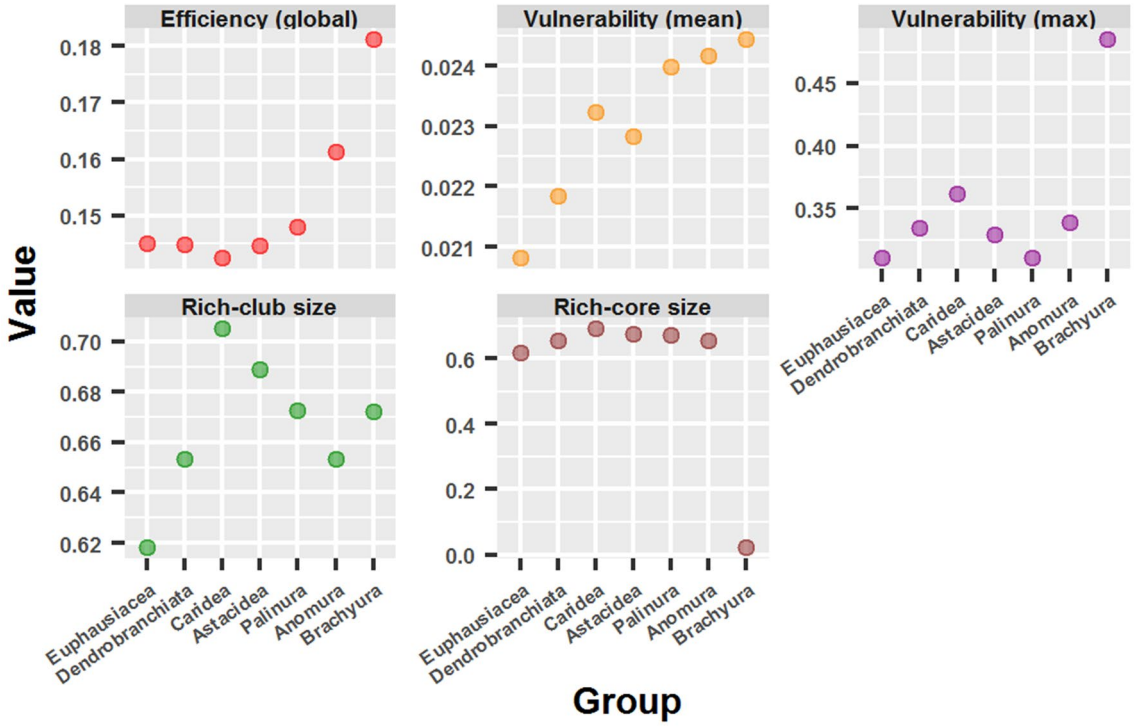

Fig. 11 Vulnerability, protection and controllability in eucaridan evolutionary networks

Vulnerability, Protection and Controllability

The efficiency of a network can be measured as how efficiently information is exchange over the network, which is inversely proportional to the shortest path between every pair of nodes (Latora and Marchiori 2001). The vulnerability of a network can be defined as the relative drop in the global efficiency when a given node is removed (Latora and Marchiori 2005). This analysis permits to predict the main targets to protect from attacks, which not necessarily are the most connected nodes (hubs).

The global efficiency, defined as mentioned above, increased exponentially during the evolution of Eucarida (24.9%) (Fig. 11). From Euphausiacea to Palinura, the efficiency remained relatively stable and then it increased abruptly in Anomura and Brachyura. The network vulnerability also increased during evolution. The mean vulnerability increased (17.4%) gradually and steadily, except for a small decrease in Astacidea. On the other hand, the maximum vulnerability remained low and stable, except for a small increase in Caridea, up to Anomura, and raised up abruptly in Brachyura (56.2%). This dissimilar behavior between the mean and maximum vulnerability was attributed to the presence of two hyper-vulnerable nodes in Brachyura, which corresponded to the cephalon (0.464) and the fused thoracomere 1–4 (0.485).

The vertiginous increase in maximum vulnerability in Brachyura pointed to a dramatic topological reorganization in this group, and to the appearance of a highly nuclear structure. To analyze this, a rich-club and rich-core analysis were performed over the evolutionary network series (Fig. 11). From Euphausiacea to Anomura, both analyses gave nearly identical results. They registered a mild increase from Euphausiacea to Caridea (14.1%), and a subsequent decrease to an intermediate value. However, in the transition from Anomura to Brachyura, while the rich-club remained at similar levels than in the previous cases (0.672), the rich-core registered an outstanding decrease in size (0.023), which meant a 96.5% reduction. Therefore, it was certain to affirm that in Brachyura the presence of a small rich-core structure was the responsible for both the high vulnerability and efficiency of the network. It is known that a large core makes a network more flexible and adaptable to changes, whereas a small core makes a network more controllable (Ma and Mondragón 2015). This is the path that seems to take the evolution of Eucarida, occurring at once in the transition from Anomura to Brachyura.

Error and Attack Tolerance

An error and attack tolerance test was carried out by removing nodes of the networks (randomly or selectively,

respectively) and measuring their respective loss of connectivity (Albert et al. 2000).

Three different approaches were used for testing attack tolerance. In the first scenario, nodes were removed in decreasing order of their degree. In the second case, nodes were removed in decreasing order of their betweenness. In the third case, a cascading approach was used, where betweenness was recalculated after the removal of each node.

The evolution from Euphausiacea to Anomura was marked by an increase in tolerance to attacks by decreasing order of degree, at fraction of nodes removed higher than 0.02 (Fig. 12a). The only exception to this behavior was Caridea, that evidenced a lower tolerance to attacks than Euphausiacea. On the other hand, Brachyura did not continue this tendency and represented the group most susceptible to attacks by decreasing order of degree.

In the case of removal of nodes by decreasing order of betweenness (Fig. 12b), the first five groups (Euphausiacea, Dendrobranchiata, Caridea, Astacidea and Palinura) did not show important differences and responded similarly to the test. On the other hand, the evolution from Palinura to Brachyura was marked by a decrease in tolerance to attacks by this strategy. In this manner, Anomura appeared as more susceptible to attacks than its predecessors. The same happened to Brachyura with respect to Anomura.

As in the first case, the evolution from Euphausiacea to Anomura was marked by an increase in tolerance to attacks by a cascading approach (Fig. 12c). Again, Brachyura departed from this tendency and represented the group most susceptible to this type of attack.

When nodes were removed randomly, that is, when tolerance to errors was tested, a different scenario was presented (Fig. 12d). The first five groups did not show significant differences in their response. On the other hand, the evolution from Palinura to Brachyura was marked by an increase in tolerance to errors. In this manner, Anomura appeared as more tolerant than Palinura and its predecessors. Meanwhile, Brachyura appeared as the group more tolerant to errors in the whole evolutionary series.

In general terms, therefore, it can be affirmed that eucaridan evolution was characterized by a decrease in tolerance to attacks and an increase in tolerance to errors, especially taking into account the initial and final conditions (Euphausiacea and Brachyura, respectively). However, there were cases where a transitory increase in tolerance to attacks was detected, such as in Palinura and Anomura in the degree and cascading scenarios.

Discussion

What is It Like to be a Crab?

Two events seemed to characterize the evolution of the superorder Eucarida analyzed using complex networks: (1) a decrease in the predominance of the carapace and (2) a reduction of the abdomen or pleon. Along the whole evolutionary process, the carapace suffered a reduction in its degree and betweenness centrality, and the abdomen gained closeness centrality. This could be observed in Fig. 2 as a reduction in size and red color intensity in the central node, and a reduction in blue color intensity in the region corresponding to the abdomen. The process responsible for both these events were the fusion of body (head, thoracic and abdominal) segments.

Although this description is correct, it is incomplete. The most important event in eucaridan evolution was the passage from a single-hub centralized network to a network governed by a triadic structure. This event occurred at the final evolution from Anomura to Brachyura. Although occurring at a single step, this process was being prepared progressively from the beginning of eucaridan evolution. This could be observed elegantly in Fig. 4, where the node corresponding to the carapace moved progressively from a zone of high betweenness centrality to a zone of high closeness centrality, forming an exponential curve. Meanwhile, the outperformer single node passed to a node trinity in Brachyura, establishing, therefore, that the transformation to a triadic structure occurred at once in the transition from Anomura to Brachyura.

However, the definite evidence in favor of the topological transformation into a triadic structure was obtained with the visual analysis shown in Fig. 2. There, it could be seen that in Brachyura the topological structure underwent a profound change. The single-hub centralized network led to a new topology, in which three nodes became the central core of the system. These three nodes concentrated a high betweenness centrality, but most importantly, they became a core of high closeness centrality that appeared sealed and concealed within the whole structure of the network. This fact was evidenced by the appearance of this core as a white node trinity (high closeness centrality) surrounded by a group of increasingly bluer nodes. This topology was not present in Anomura where the node corresponding to the carapace was still the predominant central node, while the node corresponding to the cephalon gained a certain prevalence, determining that the topology of this network could be defined as quasi-dyadic.

The aforementioned explanation of the outstanding event occurred at the final eucaridan evolution from Anomura to

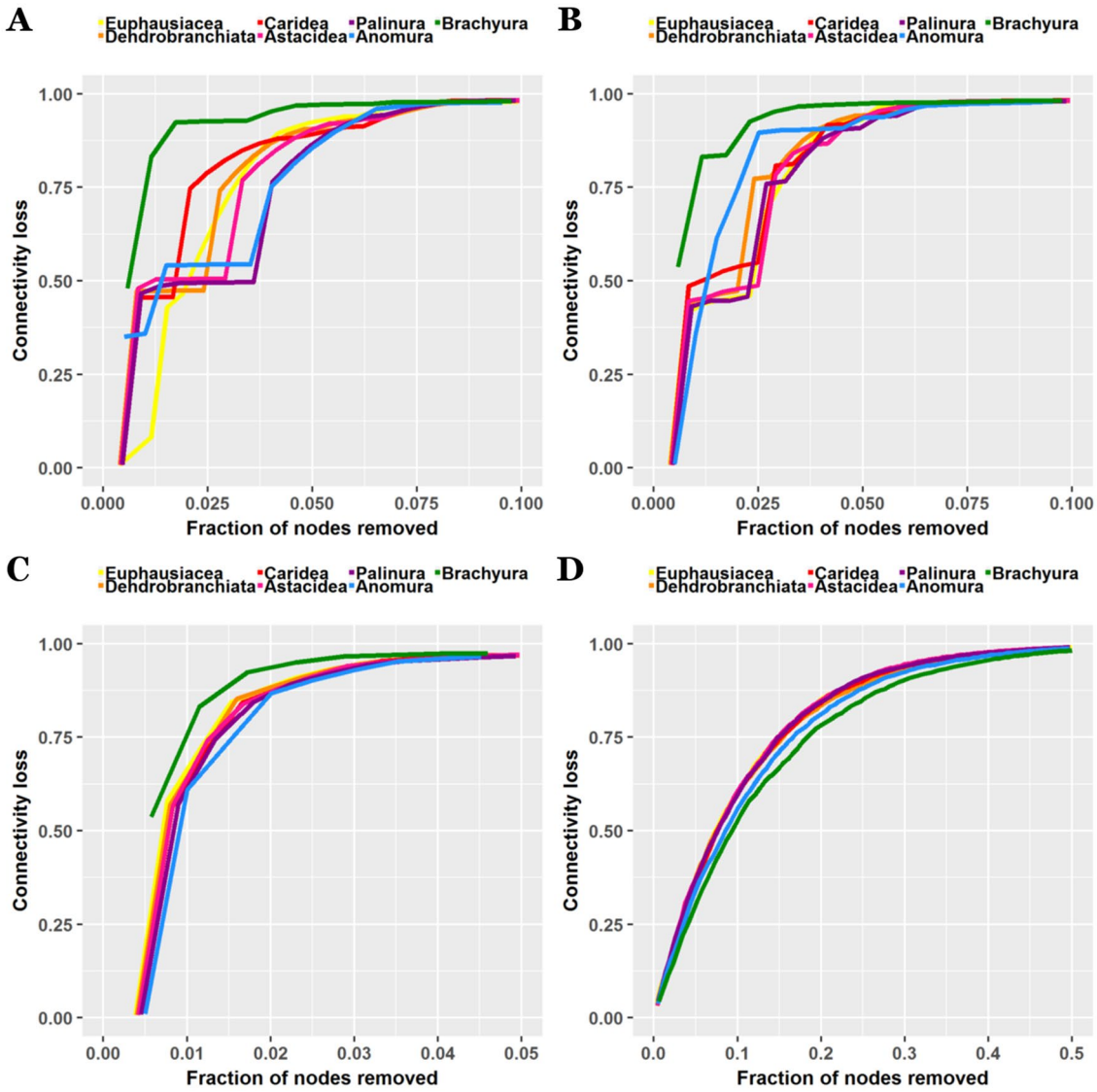

Fig. 12 Error and attack tolerance analysis. Loss of connectivity due to the removal of an increasing fraction of nodes. Nodes are removed following different criteria: **a** in a decreasing order of their degree; **b** in a decreasing order of their betweenness; **c** using a cascading scenario, where betweenness are recalculated after each node is removed; **d** randomly

Brachyura, gave us an appropriate definition of what is it like to be a crab. The definition is the following: a crab is a topological structural closure that determines the formation of a triadic central core. Therefore, the etymological analysis of the word was correct in pointing to the occurrence of a closure in the crab. However, this closure was not the "folding of the abdomen beneath the thorax", as stated by Martin and Abele (1986), but an enclosure of a triadic core within the topological structure of the network.

This conclusion was also supported by the results obtained with the rich-core analysis (Fig. 11). This analysis revealed that the evolution from Anomura to Brachyura implied a dramatic reorganization of the network topological structure, in which a relatively large rich-core size present during all eucaridan evolution led to the formation of a concentrated and nuclear small rich-core. This could be interpreted, following the conclusions stated above, as the passage from an open to a close topological structure. At the beginning, the network needed a large open core in order to govern the overall behavior of the network, whereas in Brachyura a small close core was able to govern the overall behavior. This marked the passage from an adaptable and flexible network to a controllable network. In other words, the brachyuran network became compartmentalized. Compartmentalization is associated with the presence of hierarchical organization and has been suggested to contribute to network robustness and to have an integrative function (Ma and Mondragón 2015). These conclusions are supported

by the important increase in global efficiency in Brachyura (Fig. 11).

Carcinization and Anomura as Its Last and Most Important Transitional Stage

According to our new definition of what a crab is, Brachyura was the only group that fulfilled the conditions of the definition. However, the results obtained also suggested that the process of becoming a crab began at the onset of eucaridan evolution (in the transition from Euphausiacea to Dendrobranchiata). The proof for this can be found in Fig. 4 (see the previous section for the corresponding explanation).

This gives us the opportunity to provide a proper definition of carcinization. Carcinization is going to be defined as the process of *becoming* a crab. With this definition, carcinization involves a process that includes the whole eucaridan evolution, from Euphausiacea to Brachyura, and in which the condition of a crab is only attained at Brachyura.

In spite of beginning at Euphausiacea, the process of carcinization was not even or linear in nature. Many complexity measures and topological descriptors suggested that the process accelerated at Astacidea or Palinura, after a relatively stable phase. During this process of accelerated carcinization, Palinura and Anomura represented the intermediate states between the initial and final conditions. This was especially the case for Anomura. The ZP space analysis revealed this in the clearest way. Whereas during the evolution from Euphausiacea to Palinura there was no significant change, apart from the decreasing within-module degree of the carapace, the two important novelties that characterized the brachyuran network (the connector super-hub and the non-hub hyper-connector) were already present in Anomura. The final evolution to Brachyura required the recategorization of the carapace from a local super-hub to a local hub, as well as a further increase in the participation coefficient of the three principal nodes: the cephalon, the fused thoracomere 1–4 and the carapace. Therefore, although not a crab in itself, the anomuran network showed various characteristics that were present in the crab, so it seems appropriate to affirm that Anomura represents the intermediate state *par excellence* of the process of carcinization occurring during eucaridan evolution.

Evolution Towards Complexity

Eucaridan evolution was marked by an increase in the majority of complexity measures, such as MAg, Ce, Cr, OdC and $C_{1e,spec}$. On the other hand, it was accompanied by a decrease in the majority of topological descriptors, which can be defined as extensive complexity measures, so that their decrease was explained in part by the reduction of network size during evolution.

We saw that, during evolution, the network series decreased in size and average path length, and increased in density (Fig. 1). Besides, they became more compact, less eccentric (the distance between distant node decreased), less centralized, and more interconnected (Fig. 10).

Moreover, they evolved towards structures with higher hierarchical organization (Fig. 8). It is possible that the best topological descriptor that reflected this fact quantitatively was the Balaban J index. This index increases with network size and branching (Balaban 1982), so the index raised in spite of the network size reduction. Therefore, this indicated a high increase in branching and, more deeply, in the hierarchical modular organization.

Furthermore, eucaridan evolution was accompanied by an increase vulnerability to targeted attacks and an increase tolerance to errors. This was especially true for the case of removal of nodes by decreasing order of betweenness. In the other two strategies for testing attack tolerance, by decreasing order of degree and in a cascading scenario, where betweenness was recalculated after the removal of each node, there was seen an increase tolerance to targeted attacks during the evolution from Euphausiacea to Anomura.

The error and attack tolerance analysis, in combination with the hierarchical organization analysis, suggests the formation of different levels of organization during evolution. The deeper the level of organization, the more stable and more vulnerable to attacks and modification. The prototypic example of this, and the most important, is the triadic structure present in crabs. Suggestively, two of the nodes forming this structure (the cephalon and fused thoracomere 1–4) were the most vulnerable nodes of the whole evolutionary series, a fact that can be evidenced by the abrupt increase in the maximum network vulnerability in Brachyura (Fig. 11).

This high hierarchical organization and the presence of different levels of organization may be the best evidences of structural integration. Distance-based descriptors, such as the Wiener index, may be used for measuring integration but its scope and pertinence is limited, as it measures the distance between nodes and does not consider complex structures present in the network, such as hierarchy. As explained earlier for hierarchical organization, the Balaban J index seems to be a more appropriate descriptor for measuring integration, as in our context one thing goes hand in hand with the other. Both properties point to the presence of different levels of organization, where the superior (or deeper) levels integrate the inferior (or more superficial) ones.

All the aforementioned considerations lead us to conclude that eucaridan evolution follows a trajectory that leads to a higher complexity. The formation of a triadic structure in Brachyura with high closeness centrality determined the compartmentalization of the network, which made it more controllable. This controllability derived from the hierarchical modular organization of the network, and the

concomitant formation of different levels of organization, which contributed to the development of a highly integrated structure.

Evolution Towards Robustness

Complex networks rely for their function and performance on their robustness, that is, the ability to cope with perturbations and survive accidental events.

One way of measuring robustness is by measuring network efficiency, understood as how efficiently information is exchanged over the network (Latora and Marchiori 2001). The results obtained in this work regarding network efficiency support the conclusion that robustness increased during eucaridan evolution. The efficiency (global) of the evolutionary network series increased from Palinura to Brachyura, the latter being the most efficient network (Fig. 11).

Another way of measuring robustness is by evaluating the network connectivity loss after the accidental (random) removal of nodes (Albert et al. 2000). The results obtained in this work regarding error and attack tolerance also support the conclusion that robustness increased during eucaridan evolution. Tolerance to errors and accidental events, simulated by random removal of nodes, increased from Palinura to Brachyura, the latter being the most tolerant to errors (Fig. 12).

Another potential tool for the assessment of robustness (as well as complexity) is the Laplacian Estrada index. Whereas the Estrada index is calculated with the eigenvalues of the adjacency matrix and is known to be a network centrality measure (Estrada and Rodriguez-Velazquez 2005), the Laplacian spectrum appears to be suitable for the study of the expanding properties of networks (Mohar 1991). Expanders are robust networks with high tolerance to errors due to their high connectivity properties. In this work we saw that the Estrada index decreased during eucaridan evolution, following a similar pattern as the one registered for the centralization index, proving that this property decreased during evolution (Fig. 10). On the other hand, the Laplacian Estrada index had a complex behavior which was, in great extent, the opposite to the one registered for the number of communities (Fig. 5). It is known that the second largest Laplacian eigenvalue is related to the modularity of the network (Agliari and Tavani 2017). Moreover, the spectral gap, the smallest non-zero Laplacian eigenvalue, is related to the partitioning properties of the network. A network with a small spectral gap requires a few nodes to be cut in order to generate a bipartition. Then, a small spectral gap characterizes highly modular non-hierarchical networks. On the other hand, networks with a high spectral gap are networks with high synchronizability and high spreading efficiency, that is, they exhibit a rapid and fluent dissemination and transmission of information. Therefore, a high Laplacian Estrada index is showing the formation of a network topology of this kind. The eucaridan evolution seems to imply a transitional phase with poor synchronizability and dissemination of information, but in order to arrive at a highly integrated and expandable topology in Brachyura.

Crustacean Morphology and Complex Networks

In this work, crustacean external morphology was abstracted as a network in which each individual morphological feature was considered as a node, and the edges among these nodes were established based on their physical connections. This representation and abstraction of the crustacean morphology as a network is considered to capture the evolutionary and developmental structural information of the whole organism. It represents the characteristic morphological structural framework of a given organism, its architectural plan or *Bauplan*. Each eucaridan group studied in this work had its own particular and characteristic structural plan.

The analysis of these different and successive structural plans yielded important results regarding the evolutionary trend of this group. In summary, this evolutionary trend was characterized by an increase in complexity, integration and robustness. Therefore, these models or abstractions of the crustacean morphology as networks, representing their respective structural plans or *Baupläne*, and their analysis through complex network theory, revealed important, unexpected and surprising features of their evolutionary process.

The use of complex networks, and the analysis of connectivity patterns, allowed studying an organism's morphology as a structural organization that has different hierarchical levels, topological regions and modularity values, which together determine the level of complexity, integration and robustness of the biological system. It represents a systemic and structural approach to the study of the biological processes underlying crustacean evolution. This approach is particularly relevant and suitable for crustaceans, since, like all arthropods, they are segmented animals.

From this perspective, form consists of a pattern of interconnection of parts, and the morphological and evolutionary significance of each part does not derive from its position in a three-dimensional space, but from its number of connections and from the overall pattern of interconnections of the whole system.

Acknowledgements This work was supported by a postdoctoral fellowship from Fundación Bunge y Born (FByB, Argentina). I would like to thank the academic support from Irina Podgorny (Museo de La Plata, Universidad Nacional de La Plata, Argentina), who made possible my application to the aforementioned fellowship. I would also like to thank the anonymous reviewers of this manuscript for their constructive suggestions which led to an important improvement of this article.

Compliance with ethical standards

Competing interests I declare that I have no competing interests.

References

Agliari, E., & Tavani, F. (2017). The exact Laplacian spectrum for the Dyson hierarchical network. *Scientific Reports*, *7*(39), 962.

Albert, R., Jeong, H., & Barabási, A.-L. (2000). Error and attack tolerance of complex networks. *Nature*, *406*(6794), 378–382.

Balaban, A., & Balaban, T.-S. (1991). New vertex invariants and topological indices of chemical graphs based on information on distances. *Journal of Mathematical Chemistry*, *8*(1), 383–397.

Balaban, A. T. (1982). Highly discriminating distance-based topological index. *Chemical Physics Letters*, *89*(5), 399–404.

Bastian, M., Heymann, S., & Jacomy, M. (2009). Gephi: An open source software for exploring and manipulating networks. In *Proceedings of the third international ICWSM conference* (Vol. 8, pp. 361–362).

Berkeley, A. A. (1928). The musculature of *Pandalus danae* Stimpson. *Transactions of the Royal Canadian Institute*, *16*(36), 181–231.

Bertz, S. H. (1981). The first general index of molecular complexity. *Journal of the American Chemical Society*, *103*(12), 3599–3601.

Blondel, V., Guillaume, J.-L., Lambiotte, R., & Lefebvre, E. (2008). Fast unfolding of communities in large networks. *Journal of Statistical Mechanics Theory and Experiment*, *2008*(10), 10008.

Boccaletti, S., Latora, V., Moreno, Y., Chavez, M., & Hwang, D.-U. (2006). Complex networks: Structure and dynamics. *Physics Reports*, *424*(4), 175–308.

Bonchev, D. (1983). *Information theoretic indices for characterization of chemical structures*. Letchworth: Research Studies Press.

Bonchev, D., Mekenyan, O., & Trinajstić, N. (1981). Isomer discrimination by topological information approach. *Journal of Computational Chemistry*, *2*(2), 127–148.

Bonchev, D., & Rouvray, D. (2005). *Complexity in chemistry, biology, and ecology*. New York: Springer.

Bonchev, D., & Trinajstić, N. (1977). Information theory, distance matrix, and molecular branching. *The Journal of Chemical Physics*, *67*(10), 4517–4533.

Borradaile, L. A. (1916). Crustacea. Part II. *Porcellanopagurus*: An instance of carcinization. British Antarctic ("Terra Nova") Expedition, 1910. *Natural History Report Zoology*, *3*(3), 111–126.

Claussen, J. C. (2007). Offdiagonal complexity: A computationally quick complexity measure for graphs and networks. *Physica A: Statistical Mechanics and its Applications*, *375*(1), 365–373.

Cochran, D. M. (1935). The skeletal musculature of the blue crab, *Callinectes sapidus* Rathbun. *Smithsonian Miscellaneous Collections*, *92*(9), 1–76.

Csárdi, G., & Nepusz, T. (2006). The igraph software package for complex network research. *InterJournal, Complex Systems*, *1695*(5), 1–9.

Davie, P. J., Guinot, D., & Ng, P. K. (2015). Anatomy and functional morphology of Brachyura. In P. Castro, P. J. Davie, D. Guinot, F. R. Schram, & C. Vaupel Klein (Eds.), *Treatise on zoology—anatomy, taxonomy, biology. The Crustacea* (Vol. 9C-1, pp. 11–164). Leiden: Brill.

Dehmer, M., Emmert-Streib, F., & Shi, Y. (2017). Quantitative graph theory: A new branch of graph theory and network science. *Information Sciences*, *418*, 575–580.

Dixon, C. J., Ahyong, S. T., & Schram, F. R. (2003). A new hypothesis of decapod phylogeny. *Crustaceana*, *76*(8), 935–975.

Doyle, J., & Graver, J. (1977). Mean distance in a graph. *Discrete Mathematics*, *17*(2), 147–154.

Esteve-Altava, B., Diogo, R., Smith, C., Boughner, J. C., & Rasskin-Gutman, D. (2015). Anatomical networks reveal the musculoskeletal modularity of the human head. *Scientific Reports*, *5*, 8298.

Esteve-Altava, B., Marugán-Lobón, J., Botella, H., Bastir, M., & Rasskin-Gutman, D. (2013b). Grist for Riedl's mill: A network model perspective on the integration and modularity of the human skull. *Journal of Experimental Zoology Part B: Molecular and Developmental Evolution*, *320*(8), 489–500.

Esteve-Altava, B., Marugán-Lobón, J., Botella, H., & Rasskin-Gutman, D. (2013a). Structural constraints in the evolution of the tetrapod skull complexity: Williston's law revisited using network models. *Evolutionary Biology*, *40*(2), 209–219.

Estrada, E., & Rodriguez-Velazquez, J. (2005). Subgraph centrality in complex networks. *Physical Review E*, *71*(5), 056,103.

Freitag, H. (2012). Revision of the genus *Insulamon* Ng & Takeda, 1992 (Crustacea: Decapoda: Potamidae) with description of four new species. *The Raffles Bulletin of Zoology*, *60*(1), 37–55.

Garm, A. (2004). Mechanical functions of setae from the mouth apparatus of seven species of decapod crustaceans. *Journal of Morphology*, *260*(1), 85–100.

Garm, A., Hallberg, E., & Høeg, J. T. (2003). Role of maxilla 2 and its setae during feeding in the shrimp *Palaemon adspersus* (Crustacea: Decapoda). *The Biological Bulletin*, *204*(2), 126–137.

Guimera, R., & Amaral, L. A. N. (2005). Functional cartography of complex metabolic networks. *Nature*, *433*(7028), 895–900.

Gutman, I., & Zhou, B. (2006). Laplacian energy of a graph. *Linear Algebra and Its Applications*, *414*(1), 29–37.

Huxley, T. H. (1880). *The crayfish: An introduction to the study of zoology*. London: Kegan Paul.

Ihaka, R., & Gentleman, R. (1996). R: A language for data analysis and graphics. *Journal of Computational and Graphical Statistics*, *5*(3), 299–314.

Kim, J., & Wilhelm, T. (2008). What is a complex graph? *Physica A: Statistical Mechanics and Its Applications*, *387*(11), 2637–2652.

Konstantinova, E. V., Skorobogatov, V. A., & Vidyuk, M. V. (2003). Applications of information theory in chemical graph theory. *Indian Journal of Chemistry*, *42A*(6), 1227–1240.

Langfelder, P., & Horvath, S. (2008). WGCNA: An R package for weighted correlation network analysis. *BMC Bioinformatics*, *9*(1), 559.

Latora, V., & Marchiori, M. (2001). Efficient behavior of small-world networks. *Physical Review Letters*, *87*(19), 198,701.

Latora, V., & Marchiori, M. (2005). Vulnerability and protection of infrastructure networks. *Physical Review E*, *71*(1), 015,103.

Lavalli, K. L., & Factor, J. R. (1992). Functional morphology of the mouthparts of juvenile lobsters, *Homarus americanus* (Decapoda: Nephropidae), and comparison with the larval stages. *Journal of Crustacean Biology*, *12*(3), 467–510.

Lavalli, K. L., & Spanier, E. (2010). Infraorder Palinura Latreille, 1802. In F. R. Schram & C. Vaupel Klein (Eds.), *Treatise on zoology—anatomy, taxonomy, biology. The Crustacea* (Vol. 9A, pp. 425–532). Leiden: Brill.

Lhomme, S. (2015). NetSwan: Network strengths and weaknesses analysis. R Package version 0.1.

Ma, A., & Mondragón, R. J. (2015). Rich-cores in networks. *PLoS ONE*, *10*(3), e0119,678.

Maas, A., & Waloszek, D. (2001). Larval development of *Euphausia superba* Dana, 1852 and a phylogenetic analysis of the Euphausiacea. *Hydrobiologia*, *448*(1), 143–169.

Martin, J. W., & Abele, L. G. (1986). Phylogenetic relationships of the genus *Aegla* (Decapoda: Anomura: Aeglidae), with comments on anomuran phylogeny. *Journal of Crustacean Biology*, *6*(3), 576–616.

Martin, J. W., & Abele, L. G. (1988). External morphology of the genus *Aegla* (Crustacea, Anomura, Aeglidae). *Smithsonian Contributions to Zoology*, *453*, 1–46.

Mason, O., & Verwoerd, M. (2007). Graph theory and networks in biology. *IET Systems Biology*, *1*(2), 89–119.

McLaughlin, P . A., & Lemaitre, R. (1997). Carcinization in the Anomura—fact or fiction? I. Evidence from adult morphology. *Contributions to Zoology*, *67*(2), 79–123.

Mohar, B. (1991). The Laplacian spectrum of graphs. In Y. Alavi, G. Chartrand, O. Oellermann, & A. Schwenk (Eds.), *Graph theory, combinatorics, and applications* (Vol. 2, pp. 871–898). New York: Wiley.

Moraes, J. C., & Bueno, S Ld S. (2015). Description of the newly-hatched juvenile of *Aegla perobae* (Crustacea: Decapoda: Aeglidae). *Zootaxa*, *3973*(3), 491–510.

Mowshowitz, A. (1968). Entropy and the complexity of graphs: I. An index of the relative complexity of a graph. *The Bulletin of Mathematical Biophysics*, *30*(1), 175–204.

Mueller, L., Kugler, K., Dander, A., Graber, A., & Dehmer, M. (2011). QuACN: An R package for analyzing complex biological networks quantitatively. *Bioinformatics*, *27*(1), 140–141.

Mueller, L. A., Schutte, M., Kugler, K. G., & Dehmer, M. (2014). QuACN: Quantitative analyze of complex networks. R Package Version 1.6.

Newman, M. (2003). The structure and function of complex networks. *SIAM Review*, *45*(2), 167–256.

Newman, M., & Girvan, M. (2004). Finding and evaluating community structure in networks. *Physical Review E*, *69*(2), 026,113.

Nikolić, S., Kovačević, G., Miličević, A., & Trinajstić, N. (2003). The Zagreb indices 30 years after. *Croatica Chemica Acta*, *76*(2), 113–124.

Parker, T. J., & Rich J. G. (1893). Observations on the myology of *Palinurus edwardsii*, Hutton. In: J. J. Fletcher (Ed.), Macleay Memorial Volume (pp. 159–178). Sydney: Linnean Society of New South Wales.

R Development Core Team. (2012). R: A language and environment for statistical computing. R Foundation for Statistical Computing, Vienna.

Randić, M. (1975). Characterization of molecular branching. *Journal of the American Chemical Society*, *97*(23), 6609–6615.

Rashevsky, N. (1955). Life, information theory, and topology. *Bulletin of Mathematical Biology*, *17*(3), 229–235.

Rasskin-Gutman, D., & Buscalioni, A. D. (2001). Theoretical morphology of the archosaur (Reptilia: Diapsida) pelvic girdle. *Paleobiology*, *27*(1), 59–78.

Rasskin-Gutman, D., & Esteve-Altava, B. (2014). Connecting the dots: Anatomical network analysis in morphological EvoDevo. *Biological Theory*, *9*(2), 178–193.

Ravasz, E., Somera, A. L., Mongru, D., Oltvai, Z., & Barabási, A.-L. (2002). Hierarchical organization of modularity in metabolic networks. *Science*, *297*(5586), 1551–1555.

Scholtz, G. (2014). Evolution of crabs—history and deconstruction of a prime example of convergence. *Contributions to Zoology*, *83*(2), 87–105.

Skorobogatov, V. A., & Dobrynin, A. A. (1988). Metric analysis of graphs. *MATCH Communications in Mathematical and in Computer Chemistry*, *23*, 105–151.

Snodgrass, R. E. (1950). Comparative studies on the jaws of mandibulate arthropods. *Smithsonian Miscellaneous Collections*, *116*(1), 1–85.

Spiridonov, V., & Casanova, B. (1852). Order Euphausiacea Dana, 1852. In F. R. Schram & C. Vaupel Klein (Eds.), *Treatise on zoology—anatomy, taxonomy, biology. The Crustacea* (Vol. 9A, pp. 5–82). Leiden: Brill.

Thoma, B. P., Ng, P. K., & Felder, D. L. (2012). Review of the family Platyxanthidae Guinot, 1977 (Crustacea, Decapoda, Brachyura, Eriphioidea), with the description of a new genus and a key to genera and species. *Zootaxa*, *3498*(1), 1–23.

Tudge, C. C., Asakura, A., & Ahyong, S. T. (2012). Infraorder Anomura MacLeay, 1838. In F. R. Schram & C. Vaupel Klein (Eds.), *Treatise on zoology–anatomy, taxonomy, biology. The Crustacea* (Vol. 9B, pp. 221–333). Leiden: Brill.

Wahle, R. A., Tshudy, D., Cobb, J. S., Factor, J., & Jaini, M. (2012). Infraorder Astacidea Latreille, 1802 PP: The marine clawed lobsters. In F. R. Schram & C. Vaupel Klein (Eds.), *Treatise on zoology—anatomy, taxonomy, biology. The Crustacea* (Vol. 9B, pp. 3–108). Leiden: Brill.

Watson, C. (2017). brainGraph: graph theory analysis of brain MRI data.

Wiener, H. (1947). Structural determination of paraffin boiling points. *Journal of the American Chemical Society*, *69*(1), 17–20.

Young, J. (1959). Morphology of the white shrimp *Penaeus setiferus* (Linnaeus 1758). *Fishery Bulletin*, *145*, 1–168.